Tribology of Self-Lubricating Metal Matrix Composites

2

Yinyin Zhang and Richard R. Chromik

Contents

Y. Zhang · R. R. Chromik (✉)
Department of Mining and Materials Engineering, McGill University, Montreal, QC, Canada

P. L. Menezes et al. (eds.), *Self-Lubricating Composites*,
https://doi.org/10.1007/978-3-662-64243-6_2

Abstract

Self-lubricating metal matrix composites (SLMMCs) are a class of materials that have potential to help engineers meet the demands of global initiatives for green manufacturing and sustainability. While SLMMCs have existed for many decades with traditional lubricant materials like graphite and other lamellar solids, such as MoS_2, WS_2, h-BN and CaF_2, BaF_2, scientists have recently incorporated nanostructured versions of the materials (e.g., carbon nanotubes and graphene). At the same time, new manufacturing and processing techniques have come online, such as additive manufacturing techniques that may provide significant innovation for SLMMCs. In this chapter, the current state of SLMMC research is reviewed, including materials, processing methods, and tribological performance. Processing and property relationships are described, such as influence of testing parameters and content of solid lubricants on friction and wear. Improvements in tribological behavior, as much as possible, are interpreted through third-body approach, which emphasizes materials phenomena at the sliding interface – including mechanical, structural, and chemical changes to the parent materials. Based on the review of SLMMCs and their tribology, recommendations for future research are made that emphasize the use of new materials, new processing routes, and research approaches that seek to reveal more completely the mechanisms by which these materials form tribofilms that are effective at lowering friction and reducing wear.

2.1 Introduction

Modern technology has placed materials into increasingly demanding and harsh environments. To meet the needs of next-generation applications, scientists and engineers are tasked with designing new materials with sufficient life cycle and reliability. Higher forces, temperatures, and exposure to environmental corrosion and mechanical wear lead to the need for various design strategies involving increased mechanical properties both in the bulk and at the surface. One such strategy that can be used for both surface and bulk enhancement of properties is use of composite materials.

Composite materials make use of more than one material class with one acting as the matrix and the other as a reinforcing component. Historically, composites have been used for thousands of years, with the very first examples being mud and straw composites used for housing in Egypt and Mesopotamia (circa 1500 BC) [1]. Modern engineering composites can be found nearly everywhere in our daily life, with the most common variety being polymer matrix composites (PMC) used, for example, as bicycle frames, hockey sticks, and airframe materials. More often than not, modern composites are designed from a mechanical properties perspective, where the matrix alone does not have adequate strength and/or stiffness for the design requirements. The reinforcing component, which in the PMC example is often a glass or ceramic material, enhances mechanical properties by a load transfer or load-sharing mechanism. Alongside the development of PMCs, scientists and engineers developed metal-matrix composites (MMCs). Technologies to fabricate MMCs were

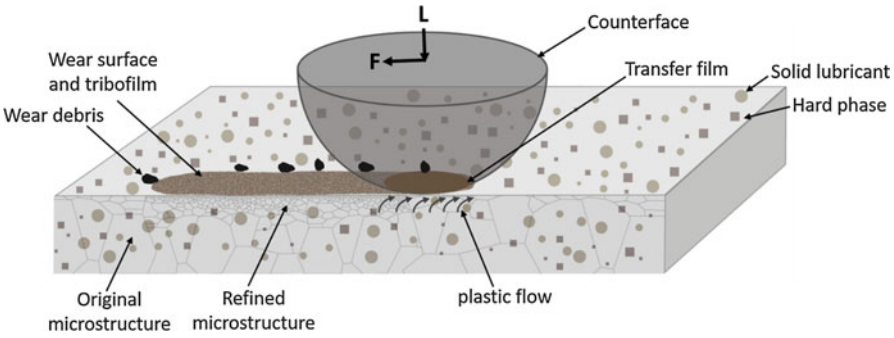

Fig. 2.1 A schematic of a bulk SLMMC that are under service. Solid lubricant–related tribofilms and, in some cases, transfer films are formed. Sliding usually generates refined microstructure on the subsurface of the wear track, and the plastic flow, shown as arrows underneath the counterface, promotes solid lubricant particles squeezing out to replenish the tribofilm and the transfer film

developed in the 1970s with increasing adoption of these materials in various applications in the following decades [2, 3]. Reinforcing components in MMCs can take the form of hard materials such as ceramics or glasses, but may also be materials for enhancement of the surface properties, known as solid lubricants.

Composite materials are often employed for tribological applications, where wear resistance and control of friction are important. Self-lubricating metal matrix composites (SLMMCs) may be in the form of bulk composites [4, 5], thick coatings or claddings [6], or thin nanocomposite coatings [7, 8]. Figure 2.1 depicts the scenarios of a bulk SLMMC that contains solid lubricants to modify friction and hard phases to support load and reduce wear. Common hard ceramic phases are Al_2O_3 and SiC and common solid lubricants are graphite (Gr), MoS_2, h-BN, and many others. The latter impart "self-lubricating" (sometimes "auto-lubricating") properties to the MMC by the formation of lubricating tribofilms and, in some cases, transfer films at the contact that can be regenerated during in-service wear of the component. Here, tribofilm refers to a surface modified layer on the material being tested and transfer films refer to a modified layer attached to the counterface (as depicted in Fig. 2.1). SLMMCs are an important class of materials for future green manufacturing and engineering sustainability. Use of SLMMCs reduces the need for oil lubrication and reduces friction and thus the energy consumption in the systems where they are used. They can also mitigate wear and increase the lifetime of components.

2.2 Selected Tribology Concepts for Metals, Solid Lubricants, and SLMMCs

2.2.1 Third Bodies for Metals and Solid Lubricants

When two surfaces are brought together to form a sliding contact, mechanical and chemical interactions lead to the formation of what tribologists commonly refer to as "third bodies" [9, 10]. The characteristics of third bodies are dictated by the

parent materials (the two "first bodies" sliding against one another), the ambient environment and parameters such as load and sliding velocity. Once the third bodies form, their behavior in the tribological system often has a significant role in determining the friction and wear performance. As shown in Fig. 2.1, transfer films may form on the ball (i.e., "countersurface" or "counterface" material) due to adhesive wear processes. Tribofilms may form on the test material of interest. They may be due to mechanical and chemical modification of the parent material but may also be due to redeposition of transfer film material to the worn surface. Wear debris is third body material that leaves the contact and no longer participates in the sliding process. There are many other names given to third bodies in the open literature, including but not limited to mechanically mixed layers (MML), tribologically transformed structures (TTS), tribomaterial, transfer layer, fragmented layer, highly deformed layer, glaze layer, white-etching layer, and nanocrystal layer [11]. MML is a common terminology in metals tribology where work-hardened, nanocrystalline, and other transformed microstructures are found at the surface [12]. TTS is a terminology used to describe nascent materials that are about to leave the first body to become part of the third bodies in the contact [13, 14]. For this chapter, we restrict discussion to "transfer films," "tribofilms," and "wear debris" – three distinct types of third bodies as labeled in Fig. 2.1.

For decades, third bodies were studied primarily by ex situ methods, where after a laboratory scale test the first bodies were separated and the nature of these materials was examined with a variety of material characterization techniques [15]. More recently, scientists developed in situ methods that are capable of directly examining third bodies during the wear test. These techniques and the history of their development were recently reviewed by Chromik et al. [16] and Wahl and Sawyer [17]. Here we mention these techniques as they were key in demonstrating the importance of examining third body "processes" or third body "flows" and the concept of velocity accommodation [18]. This is especially true for solid lubricants [19–24], such as MoS_2 and DLC. More recently, the techniques have been used to study metals tribology [25–29], which also demonstrated the importance of third bodies in determining the performance of metals in sliding contact. The manner in which third bodies modify how velocity is accommodated between two surfaces in relative motion was described by Berthier et al., where 20 velocity accommodation mechanisms (sometimes "modes") were defined or identified based on experimental evidence [18, 30].

For the context of SLMMCs, understanding of third bodies and their formation is crucial. These materials are designed specifically to form and replenish tribofilms from the self-lubricating fillers within their matrix. The effectiveness of this process and the mechanisms by which it occurs are not always fully explored in the literature. In fact, it is only until recently that in situ tribology techniques have been applied to composite materials for nanocomposite PVD coatings [8] and MMCs [28, 29, 31]. Researchers have, however, used ex situ methods to investigate tribofilm formation on SLMMCs which have demonstrated their importance and role in lubrication and enhancement of the tribological properties [32–36]. It is also true that the nature of self-lubrication for an SLMMC is related to the same processes that occur for solid lubricant applied as coatings. However, the source flow of lubricating material is

potentially much less for an SLMMC and the third bodies that form, and their flows are expected to be substantially altered. As such it is worthwhile to have a short review of what is expected for self-lubrication when solid lubricants are applied as blanket films.

2.2.2 Solid Lubricants

Solid lubricants are a class of materials that provide a lower friction in comparison to standard tribological couples found in engineering systems, where the vast majority are metal-metal or metal-alloy type contacts [15, 37, 38]. The most popular solution is the use of oil lubrication, but in cases where this is not possible (e.g., space applications, open system), one may resort to the use of solid lubrication. The most common solid lubricants are lamellar type solids, such as Gr and a set of metal dichalcogenides (e.g., MoS_2, WS_2). However, there are many others [15] and it is also the case that soft metals (e.g., Pb, In, Au) are considered solid lubricants at elevated temperatures. All solid lubricants typically have a narrow range of effectiveness in term of environmental conditions such as temperature, humidity, and ambient pressure.

The mechanisms by which solid lubricants provide low friction are always a topic of debate. However, scientists do agree on the basic concept of an interfacial shear strength. Figure 2.2 shows schematically the concept of modifying the friction by an interfacial film with lower shear strength than the bulk solid to which it is applied. Velocity is accommodated by the solid lubricant, which could be in the form of a coating or a tribofilm formed from a SLMMC. The velocity accommodation mode (VAM) can be: (i) interfacial sliding between a transfer film and tribofilm; (ii) the counterface material and the tribofilm (absent of transfer film); (iii) interfilm shearing of the transfer film, tribofilm, or both; or (iv) interfacial sliding between the counterface and wear track (absence of tribofilm and transfer film). For a blanket

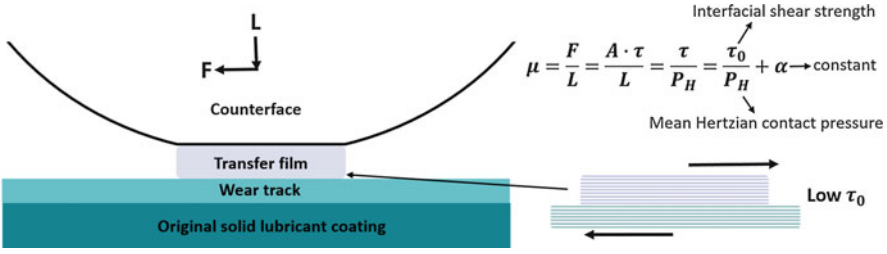

Fig. 2.2 A schematic of interfacial sliding along transfer film and wear track interface and how solid lubricants modify the friction by an interfacial film with low interfacial shear strength. The above expression for the friction coefficient is based on the classical theory of Bowden and Tabor, where friction force can be expressed as a product of real contact area (A) and shear strength of the lubricant material (τ). τ_0 is the interfacial shear strength, a "velocity accommodation parameter" which is a property of the interface, and α is the lowest attainable friction coefficient for a given friction couple [16, 38, 39]

coating of solid lubricants, the most common VAMs are (i) and (iii). For SLMMCs, where there is incomplete coverage of the wear track, all four can occur, but (ii) and (iv) are most common. Interfacial sliding of counterface versus the tribofilm is the mechanism of lubrication for SLMMCs. In the absence of solid lubricant in the tribofilm, interfacial sliding leads to higher friction, and adhesive and/or plowing wear, which provides a mechanism to release more solid lubricant materials from the subsurface of the SLMMCs.

For lubrication by carbonaceous species, there is extensive literature on diamond-like carbon coatings, which was recently summarized in [40, 41]. Carbonaceous films are quite common and also from other species such as oils, varnishes, and greases, as pointed out by Hoffman and Marks [42]. Historically, tribologists explained the lubricating effect from diamond-like carbon coatings as a "graphitization" process by which the initially amorphous coating formed tribofilms that transformed to Gr due to the temperatures and/or pressures induced by the sliding [43, 44]. Work by Scharf and Singer demonstrated the importance of formation of transfer films for a specific Si doped DLC [19, 21]. However, it is not the case that all DLC coatings behave the same way and in some cases one observes that transfer films are less important and tribofilms on the worn surface dominate the process [45]. Sometimes it is even the case that the dominant mechanism determining friction is near surface passivation state of the DLC. Recent computational simulations by Pastewka et al. [46] demonstrated that it is not always a graphitic structure that provides low friction. Sometimes it is sufficient to form sp^2 hybridized carbon from the sp^2/sp^3 matrix of the DLC coating. They also concluded that a passivation process was important for realizing low friction. Experimental observations of superlubricity in some DLC coating support these observations, where the surface termination is highly important for realizing the ultralow friction [47]. Other carbon species, such as graphene (G) or carbon nanotubes (CNTs), have been added as surface layers and resulted in lowered friction an improved tribological performance. Work by Berman et al. [48–51] has demonstrated outstanding lubricating effects by deposition of G onto metallic surfaces.

Coatings made from MoS_2 and WS_2 have been applied for many decades as solid lubricants, having been developed in the early days of the development of space technology [52]. This lamellar solid is most effective for low friction in vacuum or in the absence of humidity. Ambient conditions lead to a rise in friction and more rapid removal of the coating. The mechanism of the effect of humidity is debated in the literature, with some researchers showing evidence of the formation of Mo-oxides [53] and others demonstrating that friction between pristine MoO_3/MoS_2 interfaces is extremely small along the channel direction, which is formed by S atoms at the sliding surface, even smaller than that of MoS_2. The friction rise is due to the high energy barrier of MoO_3 (001) interlayer sliding that leads to an increase in the shear strength [54, 55]. The formation of transfer films is critical for the performance of these materials [8, 56, 57]. Recent work by Hoffman and Marks [58] demonstrated the mechanism for transfer film formation. It is also the case that even after wearing through an MoS_2 coating, low friction can persist by the presence of tribofilms and recirculation of MoS_2 debris back into the tribosystem [59]. Recent work by Lince

et al. demonstrated that other Mo-S compounds that have green manufacturing processes have promise to be as effective as MoS_2 [60]. Similar to carbon materials, MoS_2 and WS_2 have seen an evolution of their structure to make two-dimensional structure (e.g., like G) and nanoparticles/nanotubes [7, 61]. These materials have the possibility to be placed on surfaces for lubrication or added as filler materials in SLMMCs.

2.2.3 Incorporation of Solid Lubricants in MMCs

There is a long history of incorporation of solid lubricant materials into metal matrices. Graphite inclusions are the most extensively studied, with Rohatgi and coworkers carrying out much of the early work on Al-Gr composites fabricated by casting routes [2, 62–66]. Researchers have also incorporated MoS_2, WS_2, and h-BN into metals by powder metallurgy or other techniques [67–69]. Since the early years of manufacture of SLMMCs, which was primarily with casting and powder metallurgy methods, there have been significant advances in both alternative processing technologies and the materials themselves (e.g., Gr replaced by CNTs or G). In the end, regardless of processing route or material system, the fabrication of any SLMMC has a few key goals in mind. Firstly, the solid lubricant should be dispersed as homogeneously as possible and be unmodified by the processing. The actual volume fraction of the solid lubricant included is often a function of the application itself. This is because as the volume fraction of the solid lubricant increases, there is inevitably a detriment to the bulk mechanical properties. Often there may be some benefit to mechanical properties at low volume fractions, but at higher concentrations, the solid lubricant will result in softening. Thus, the second main goal is finding a balance of the lubricant content. Ideally, one requires a sufficient amount that there can be a sustainable lubricating tribofilm at the material's surface throughout its lifetime, but not so much lubricant that there is an unacceptable debit in mechanical properties. This is why one often finds SLMMCs that also include hard phases. The load-supporting nature of hard inclusions helps to overcome the debit in mechanical properties introduced by the solid lubricant. Many of the newly developed processing routes also seek to incorporate higher content of lubricant with better maintainability of mechanical properties. The remainder of this chapter will address the tribology of carbon-based and MoS_2/h-BN/WS_2/CaF_2/BaF_2 SLMMCs with special attention to the role of third bodies in determining the performance of these materials.

2.3 Synthesis of SLMMCs

Historically, Gr has been incorporated in metal matrices for many decades. This is especially true for Al and its alloys, where these materials have found applications as bearing surfaces, fan bushings and pistons and liners of internal combustion engines [4]. These materials can be fabricated in a relatively low-cost casting process [65, 70–73], infiltration techniques [63], or by powder metallurgy routes [74, 75]. More recently, newer processing methods have been developed including friction

Table 2.1 Summary of some fabrication methods for SLMMCs containing Gr, CNTs, or G

Carbon species	Fabrication method	Matrix materials	References
Gr	Stir casting	Al or Al alloy	[65, 70–73]
	Infiltration	Al or Al alloy	[63]
	Powder metallurgy	Al or Al alloy	[74, 75]
	Friction stir welding	Al or Al alloy	[76–82]
	Microwave sintering	Cu	[95]
CNTs	Powder metallurgy	Cu, Al	[99–101]
	Friction stir welding	Al or Al alloy	[76]
	Microwave sintering	Cu	[96]
	Cold spray	Cu, Al	[86–91, 102]
	Laser AM technique	Ni	[98, 103]
	Infiltration	Al	[104]
G	Sintering (spark plasma, semisolid, or laser)	Ni_3Al, Al alloy, Ti	[105–107]
	Powder metallurgy	Al	[108]
	Friction stir welding	Al or Al alloy	[76]

stir techniques [76–82], electrodeposition [83–85], thermal spray, cold spray [86–94], microwave sintering [95–97], and laser melting/additive manufacturing methods [98]. Some of these fabrication methods are more directed as fabrication of coatings (i.e., electrodeposition and thermal spray), while the remainder are directed at fabricating a bulk material. Cold spray is capable of producing coatings and also can be used as an additive manufacturing method to create near-net shape bulk parts. The manufacturing methods and materials for carbon-based lubricants were summarized in Table 2.1 according to the most recent literature, while Table 2.2 listed the most recent main techniques used for synthesis of MoS_2-, h-BN-, WS_2-, CaF_2-/BaF_2-SLMMCs. One may notice that manufacturing methods have a significant influence on material selection, microstructure of the matrix, stability of the solid lubricant reinforcement(s), as well as bonding mechanism between the matrix and the reinforcement(s). Powder metallurgy has been applied to a wide range of matrix materials such as Cu, Mg, steel, and Ni base alloy. Plasma spray and laser cladding can be used to fabricate superalloy–based composites because of high temperatures they are able to achieve. However, cold spray, due to its bonding mechanism (discussed in details later), while has been widely used for ductile metals deposition, is still under development for manufacturing superalloy coatings [119].

2.3.1 Powder Metallurgy

Powder metallurgy basically includes three steps: mixing, compacting, and sintering of mixtures consisting of matrix and reinforcement powders [64]. The current primary problems and challenges regarding fabrication of SLMMCs using powder

Table 2.2 Summary of most recent main synthesis of SLMMCs containing MoS_2, WS_2, h-BN, CaF_2, and BaF_2

Technique of synthesis	Processing temperature (°C) or material state	Matrix material	Solid lubricant(s)	Reference
Powder metallurgy	1200	Ni base alloy	Ag + h-BN	[109]
Powder metallurgy	600 and 1200	SS316L	h-BN, MoS_2	[36]
Powder metallurgy	530	Mg-TiC	MoS_2	[110]
Powder metallurgy	800	Cu-Sn	MoS_2	[111]
Plasma spray	Semi-liquid	NiCr-Cr_3C_2	h-BN	[112]
Plasma spray	Semi-liquid	WC-Co-Cu	MoS_2	[113]
Laser cladding	Liquid	Ni base alloy	WS_2	[114]
Laser cladding	Liquid	Co base alloy-TiC	CaF_2	[115]
Cold spray	Solid	Cu	MoS_2	[32, 116]
Cold spray	Solid	Ni	h-BN	[117, 118]

metallurgy are decomposition of solid lubricants due to high processing temperature, high porosity and poor bonding strength of the matrix and reinforcement(s), and manufacturing of self-lubricating MMCs for high temperature applications.

Decomposition of solid lubricants occurs because sintering temperatures are higher than oxidation or dissociation temperatures of commonly used solid lubricants, as shown in Table 2.3 [38, 120, 121]. For Cu-MoS_2 composites, sintering temperature above 780 °C causes decomposition of MoS_2 and formation of a brittle phase $CuMo_2S_3$ that is detrimental to tribological behavior [111, 122]. Figure 2.3 exhibits typical microstructure of SS316L-15 vol.% MoS_2 composite fabricated by powder metallurgy [36]. During sintering (1200 °C), MoS_2 phase was replaced by iron sulfide due to decomposition of MoS_2 and interaction with 316L. As the newly formed sulfides are not as lubricious as MoS_2 [123], some strategies have been employed to improve maintenance of solid lubricants. Adding alloying elements, i.e., phosphorus (admixed and pre-alloyed) and molybdenum (admixed), into steel matrix delayed, yet did not avoid, MoS_2 decomposition and reaction [123]. Moreover, h-BN or metal-coated h-BN was used to withstand high sintering temperature because of its high thermal and chemical stability [36, 124, 125]. However, due to the low wettability and poor sinterability, incorporation of h-BN into metal matrix led to slight decrease in mechanical property, i.e., hardness [36, 124–126]. Other solid lubricants exhibiting higher oxidation resistance could be potentially applied to stand high sintering temperatures.

Porosity and bonding strength between metal matrix and solid lubricant reinforcements are important material properties that have to take into account. Inadequate bonding occurs when sintering temperature is below melting point of

Table 2.3 Oxidation or decomposition temperatures of selected solid lubricants

	Gr	MoS_2	WS_2	h-BN	(Ca, Ba)F_2
Oxidation/°C	325	370	539	>700	~600

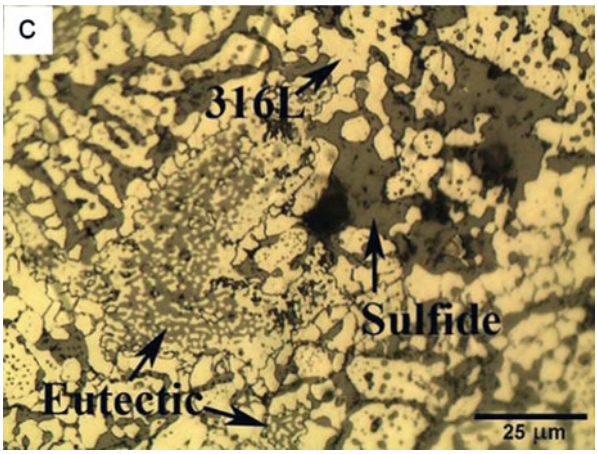

Fig. 2.3 An optical micrograph of cross section of SS316L-15 vol.% MoS_2 composite fabricated by powder metallurgy. Reprinted from [36], with permission from Elsevier

metals. In order to improve it, hot pressing, which performed sintering under a high pressure, and spark plasma sintering, which produced a high heating rate (up to 100 °C/min), were used to effectively decrease porosity and improve bonding strength [64, 127]. Glow discharge sintering is a relatively new technique that uses abnormal glow discharge plasma to generate a rapid and accurate heating process and reduce porosity [128]. Finally, post-treatment such as extrusion improved density and hardness of Cu-Sn-MoS_2 composites [123].

2.3.2 Laser Surface Cladding (LSC)

Due to a recent reduction in cost of laser equipment, researchers have devoted efforts on research and development on laser cladding process [129]. During LSC, an alloy or a composite layer is fused onto the surface under a coherent and high intensity laser beam irradiation [129]. The melt pool temperature can achieve as high as 2000 °C by using extremely high power density [129]. Critical processing parameters include mixing of the feedstock powders, heating rates, convection, diffusion, and cooling rates [129]. A significant difference between LSC and other coating techniques is its strong bond between coating and substrates due to the fact that substrate is partially melted into melt pool and participate in coating development. Therefore, there is no significant interface visible between the substrate and coating. For fabrication of self-lubricating MMCs, LSC has recently been employed to produce superalloy–based composites for high temperature applications [33, 114]. A major problem of LSC applied to solid lubricants is decomposition and

vaporization during the high temperature laser processing. It has been observed that MoS_2 dissociated and interacted with matrix materials in the melting pool [130, 131]. Xu et al. fabricated Ni-TiC-MoS_2 composite on 1045 low carbon steel using laser cladding. MoS_2 was found to be decomposed to Mo and S, resulting in the formation of $Ni_{2.5}Mo_6S_{6.7}$, intermetallic $Mo_{0.84}Ni_{0.16}$, and binary element sulfides (Ni_3S_4, NiS_2, Ni_3S_2, NiS) [130]. Generally, there are two methods to improve the decomposition. First of all, solid lubricants having higher oxidation resistance and melting points such as h-BN, WS_2, CaF_2, and BaF_2 have been observed to have a higher recovery in the final composites [33, 115, 127, 132–134]. Moreover, feedstock pretreatments such as encapsulation solid lubricants with metal by high energy milling or electroless plating reduced effectively decomposition and vaporization of solid lubricants [132, 135–137].

2.3.3 Thermal Spray

In this method, melting or semi-melting metal particles are co-sprayed with solid lubricants. Ni base alloys and WC-Co have recently been sprayed with MoS_2, h-BN, as well as (Ca, Ba)F_2 [112, 113, 139–142]. Figure 2.4 shows typical gas temperature and particle velocity of thermal spray techniques and cold spray [138]. The biggest challenge of the current thermal spray techniques is to prevent solid lubricant from decomposition and interaction to the matrix material during high temperature processing. Metal-coated solid lubricant prepared by ball milling or hydrogen reduction followed by alloying method helped to retain MoS_2 and h-BN in the composite coating [112, 113]. However, due to poor wettability of h-BN with melt metals, real interparticle contact surface and bonding strength decreased with h-BN, and 10 wt% of h-BN was found to destroy the continuity of Ni_3Al matrix [142]. Detonation gun spray, due to its relatively lower heat input and higher particle speed, could potentially minimize MoS_2 decomposition [140].

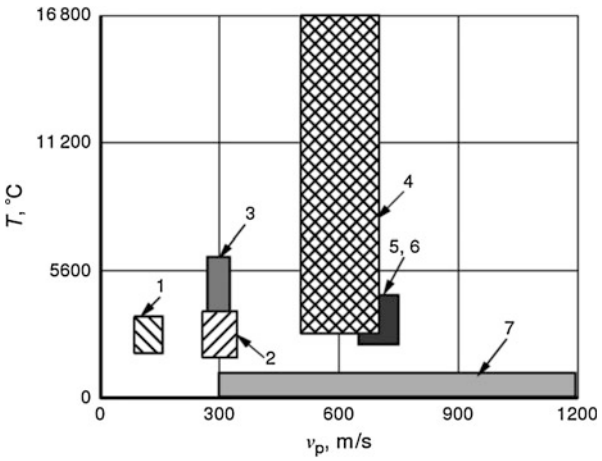

Fig. 2.4 Diagram of jet temperatures (T) and particle velocities (*v*p) used in thermal spray and cold spray methods. *1* low velocity gas plasma; *2* high velocity gas plasma; *3* electric arc; *4* plasma; *5*, *6* detonation and high velocity oxy-fuel (HVOF); and *7* cold spray. Reprinted from [138], with permission from Elsevier

2.3.4 Friction Stir Processing (FSP)

Friction stir processing (FSP) is a solid state process aiming to modify microstructures of a single or multiple workpieces and to fabricate MMCs [81, 143]. A specially designed rotating pin is inserted into the material with a proper tilt angle, and moving along the designed path. Rotation of the pin stirs the metallic surface and generate friction and plastic deformation heat, leading to a mix of the surface material (i.e., coated powder) and the metallic matrix [76, 81]. The mix then flows to the back of the pin, where it is extruded and forged behind the tool, and eventually consolidates and cools down under hydrostatic pressure conditions [81]. FSP is an excellent method to fabricate MMCs showing well-dispersed solid lubricant and/or ceramic reinforcements and improved mechanical properties [76–82]. Gr, G, CNTs, and MoS_2 have been incorporated into aluminum alloy by FSP and these composites exhibited improved mechanical property and tribological performance [76–82, 144]. Hybrid composites including solid lubricant and ceramics such as SiC and Al_2O_3 have been developed successfully by FSP on aluminum alloy surface [76–82, 144]. However, FSP has been mainly applied for aluminum MMCs so far. New applications of FSP to other metallic materials are under development [81].

2.3.5 Cold Spray

Cold spray, or cold gas-dynamic spray, is a solid state deposition process by exposing a suitable substrate to a high velocity (300–1200 m/s) jet of particles, which are generally metals or blends of metals and other materials [119, 146, 147]. The powders are accelerated by a high pressure gas jet through a de Laval nozzle [119, 146, 147]. Upon impact, the metallic particles that achieve a critical velocity undergo adiabatic shear instability, leading to metallurgical bonding, and consequently buildup of a coating [146–148]. The impact phenomenon and comparison with a wide range of other types of impact is summarized in Fig. 2.5, that points out the cold spray deposition possibly occurs within a typical particle size range of 5–150 μm at an impact velocity of 300–1200 m/s, which forms the cold spray regime [145]. Low temperature and high speed deposition make it very attractive for oxidation and heat sensitive materials and to fabricate high density composites [138, 149]. Even though cold spray has been discovered early in 1980s and successfully used for metals and metal-ceramic composites, its application to SLMMCs has just begun [146, 147, 150]. Currently, there are two main research groups including Penn State University and McGill University that have investigated cold sprayability of solid lubricants with metals. Figure 2.6 shows an optical micrograph of cold sprayed Cu-MoS_2 composite using admixed Cu and MoS_2. MoS_2 was distributed along Cu particles, and it was demonstrated that under the optimized spraying condition, average MoS_2 content in the composite was around 2–3 wt%, lower than those fabricated by some of the other techniques, e.g., around

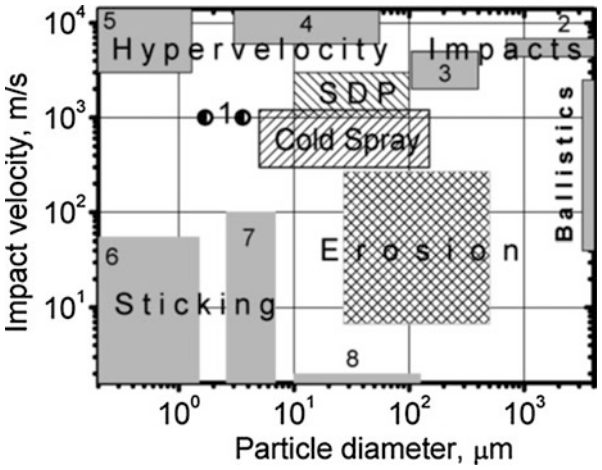

Fig. 2.5 Influence of impact velocity and particle size on material interaction upon impact of ductile metals or alloys with plane solid surfaces. Regions characteristic of impact phenomena are shown: *1*: no adhesion; *2, 3, 4,* and *5*: hypervelocity impacts; *6* and *7*: low-velocity impact; *8*: rebound; *SDP* super-deep penetration. Reprinted from [145], with permission from Elsevier Masson SAS. All rights reserved

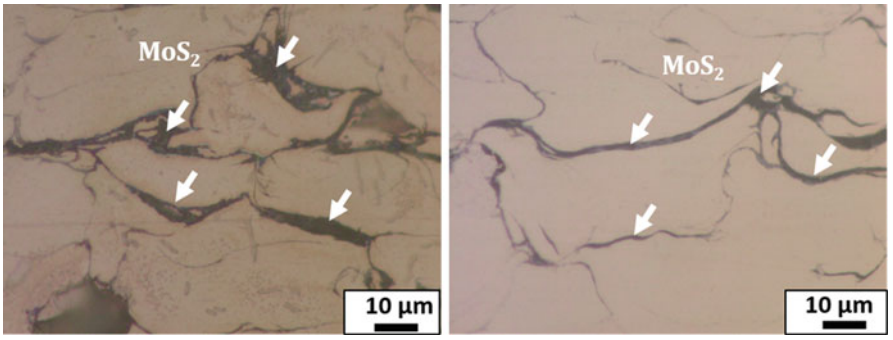

Fig. 2.6 Typical optical micrographs of cold sprayed Cu-MoS_2 composite using admixed Cu and MoS_2. Reprinted from [116], with permission from Springer

30 wt% MoS_2 can be achieved by powder metallurgy [32, 116, 133]. Deposition mechanism of Cu and MoS_2 composite during cold spray was proposed by Zhang et al. [116]. Presence of MoS_2 hindered extensive adiabatic shear instability of Cu occurring, leading to inadequate bonding between Cu particles, and therefore reduced mechanical property e.g., hardness of the composite [116]. Adding ceramic phase, e.g., WC to form hybrid composite Cu-MoS_2-WC could potentially improve mechanical property. Moreover, Ni-coated h-BN was fabricated by electroless process and used as feedstock to develop Ni-matrix h-BN composite. The size of solid lubricant core was found to play an important role on recovery of solid lubricant and bonding between particles. Nano-h-BN (100 nm) encapsulated with Ni helped to achieve around 10 vol.% h-BN retained in the composite [118, 151]. However, they observed 1 vol.% h-BN composite produced the best combination of friction and wear behavior [118, 151]. More extensive observation on bonding mechanism of the solid lubricant and metal particles, as well as its influence on tribological performance, is required.

2.4 Metal-Graphite, CNTs, Graphene SLMMCs

2.4.1 Advances in Materials (Gr → CNTs → G)

An aspect of the carbon-based SLMMCs that has changed over the years is the nature of the carbon species that is impregnated into the composite. In the early days, researchers were limited to Gr flakes as the only commercially available material. With the invention of carbon nanotubes in the 1980s followed by graphene in 2000s, there is now the possibility of including other forms of carbon in place of Gr flakes. The tribology of composites with carbon nanotubes is well researched, having been studied nearly since their invention with a recent review article published on the topic by Moghadam et al. [152]. Research on graphene-containing composites have only recently been demonstrated and carried out [82, 102, 107, 108, 153–156]. Limited information on the tribology of these materials has been published [76, 84, 85, 157–159]. However, for all of these additions, the intention is still that the carbon species will develop a tribofilm on the surface upon sliding.

2.4.2 Tribological Behavior of SLMMCs Containing Graphite, CNTs, and Graphene

The tribological behavior of Gr, CNTs, and G containing SLMMCs has been the subject of recent reviews by Omrani, Moghadam, and coworkers [4, 5, 152, 160]. Some general trends of friction and wear with material and test parameter for MMCs containing Gr are well understood, especially for Al matrices. With increasing Gr content in the composite, there is a reduction in friction coefficient. Figure 2.7a presents friction results versus Gr content for two separate studies by Akhlaghi et al. [161, 162]. Variation in the friction among the studies is related to changes in applied load and sliding velocity, but in general there is a consistent trend to lower friction with increasing Gr content. The trend is observed for the vast majority of literature on Al-Gr MMCs regardless of their method of manufacture. Similarly, for wear of the composite (see Fig. 2.7b), there is a decrease in wear with increase in the Gr content for a set of studies by Ravindran et al. and Suresha et al. [163, 164]. It should be noted that this trend is not always respected. That is, many authors have reported that as the Gr content is increased, eventually wear will increase. There is some optimum content of Gr to obtain both low friction and wear, above which wear will increase even if the low friction is maintained. This is generally related to a reduction in the mechanical properties of the composite with the increased Gr content, which can lend itself to enhance mechanical properties at low inclusion content but with large content, leads to a softening of the composite. In general, the effect can be more pronounced for composites produced by powder metallurgy as compared to those prepared by stir casting. Liu et al. prepared stir cast Al-50%Gr composites and saw a relatively good performance for both friction and wear [63]. However, for composites produced by powder metallurgy, Akhlaghi et al. observed an increasing trend in wear with increasing Gr content [4, 75].

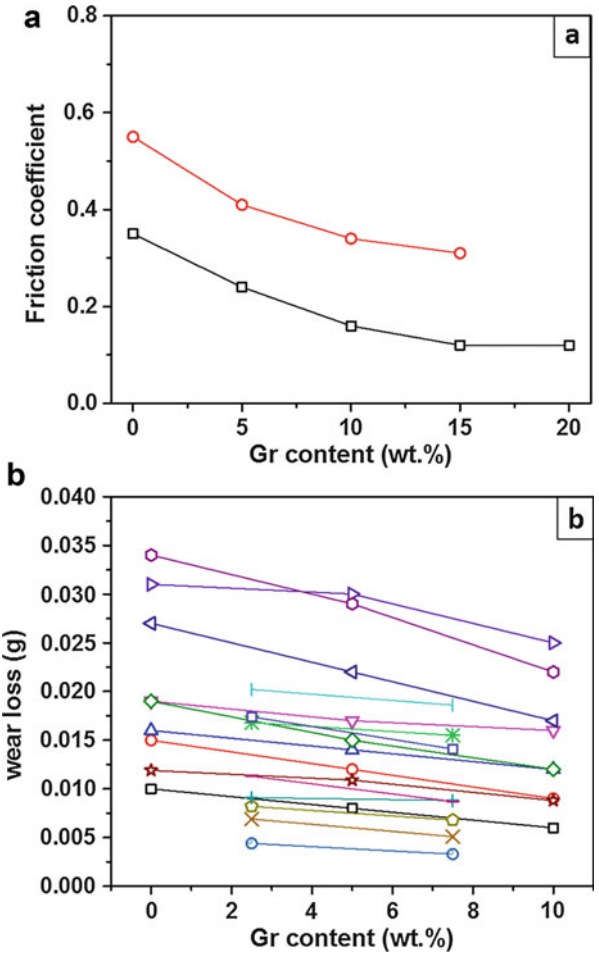

Fig. 2.7 The trends of (**a**) friction [161, 162] and (**b**) wear loss [163, 164] with Gr content in Al SLMMCs

To overcome this trend, they included SiC reinforcements to enhance the mechanical properties of the composite. This is a common strategy that can maintain acceptable wear rates at higher Gr concentrations.

More recently, researchers have mixed CNTs and G into MMCs. The remarkable mechanical properties of CNTs and friction properties of G led naturally to the research question of whether these carbonaceous reinforcements would lead to even better self-lubricating properties than Gr. Zhou et al. [104] studied the tribology of CNT in Al-Mg MMCs. Figure 2.8 demonstrated the reduction in friction and wear they observed with CNT. Similar reductions were also observed by Choi et al. on a CNT-Al composite [165]. One aspect of the inclusion of CNTs that is often not fully explored by all researchers is the state of the CNTs post-processing. Poirier et al. studied Al-CNT composites made by a mechanical milling process and discovered that nearly all of the CNTs were destroyed and had reacted to form carbides with the

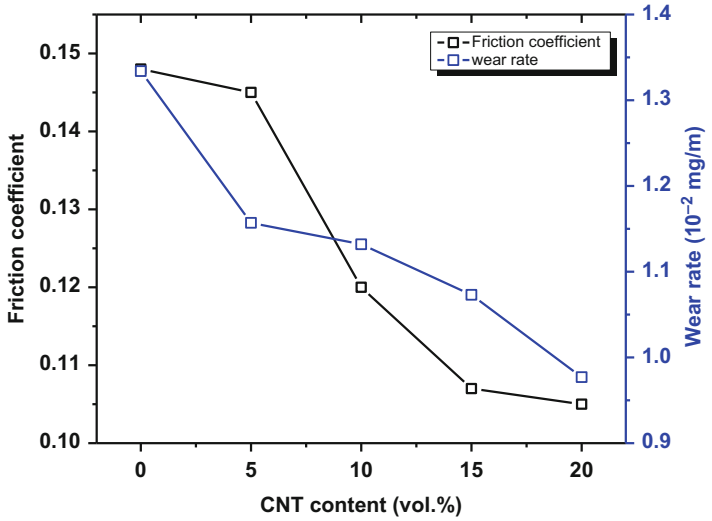

Fig. 2.8 Trends with CNT content in an Al composite made by powder metallurgy methods [104]

Al matrix [166]. Depending on the aggressiveness of the processing steps taken to create the composites, one may find retention of CNT as a distinct phase in the microstructure or instead the formation of carbides. Both Zhou et al. [104] and Choi et al. [165] showed evidence with transmission electron microscopy that nanotubes were retained in their composite in an unreacted state.

Only recently have researchers studied the inclusion of G in MMCs [76, 84, 108, 158, 167]. Ghazaly et al. [108] studied the tribology of Al-G composites and discovered the wear performance was not significantly improved. On the other hand, research on Ni-G composites showed a reduction in both friction and wear of the composite with an increase in G content [84]. Sometimes it is difficult to ascertain the effectiveness of a new materials due to differences in processing, matrix material, and test parameters. As such, it is very difficult at these early stages of G-based SLMMCs to determine whether the form of the carbon introduced in the composite affects significantly the tribological performance. However, a recent paper by Maurya et al. [76] provides a side-by-side comparison of Gr, CNT, and G reinforcements in a friction stir processed Al alloy. In Fig. 2.9, the friction trends they observed are presented. Gr and CNT additions had a similar reduction in the friction coefficient to about 0.4, while G lowered the friction to around 0.25. For the wear of the composite, they observed that all reinforcements reduced wear compared to the friction stir alloy without carbon additions. There was also a trend in wear depending on the carbon species, where G reduces the wear most followed by CNT and the least effective being Gr. While the authors conducted ex situ analysis of their wear scars, the precise mechanism of the differences in the performance of the three carbonaceous species was not identified. Future research on carbon-containing SLMMCs should certainly focus on more side-by-side comparisons between Gr, CNTs, and G.

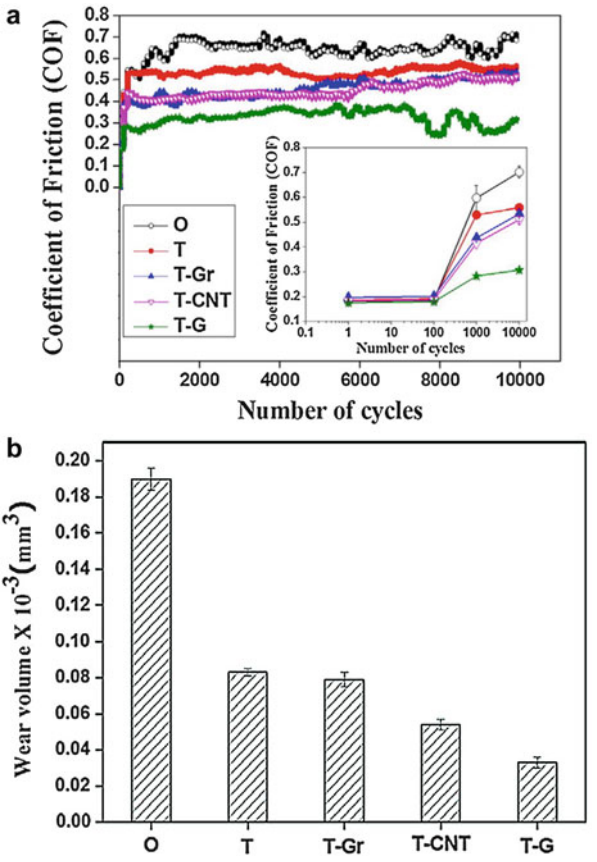

Fig. 2.9 Friction and wear trends with Gr, CNTs, and G composites made with Al6061 alloy with friction stir processing. Reprinted from [76], with permission from Elsevier

2.4.3 Tribofilms Observed for SLMMCs Containing Graphite, CNTs, or Graphene

Examination of worn surfaces after tribology testing can help to determine the wear mechanisms. In the case of SLMMCs, the comparisons between the composite and a pure version of the matrix material can explain the effectiveness of the solid lubricant in reducing friction and wear. Figure 2.10 are secondary electron images of worn surfaces on Al7075/Gr composites with increasing Gr concentration [168]. With no Gr, there is evidence of adhesive wear and plastic deformation on the worn surface. As Gr is introduced to the composite, evidence of this wear mechanism is reduced and instead a smoother worn surface with grooved features is observed. Many authors have explored the characteristics of the graphitic tribofilms formed on Al-Gr composites [63, 161, 163, 169–173]. General trends observed are that with increased Gr content in the composite, there is an enhancement of the tribofilm coverage of the surface that correlates with the reduction in friction. Interestingly, there is a significant lack of observation of the counterface materials in tribological

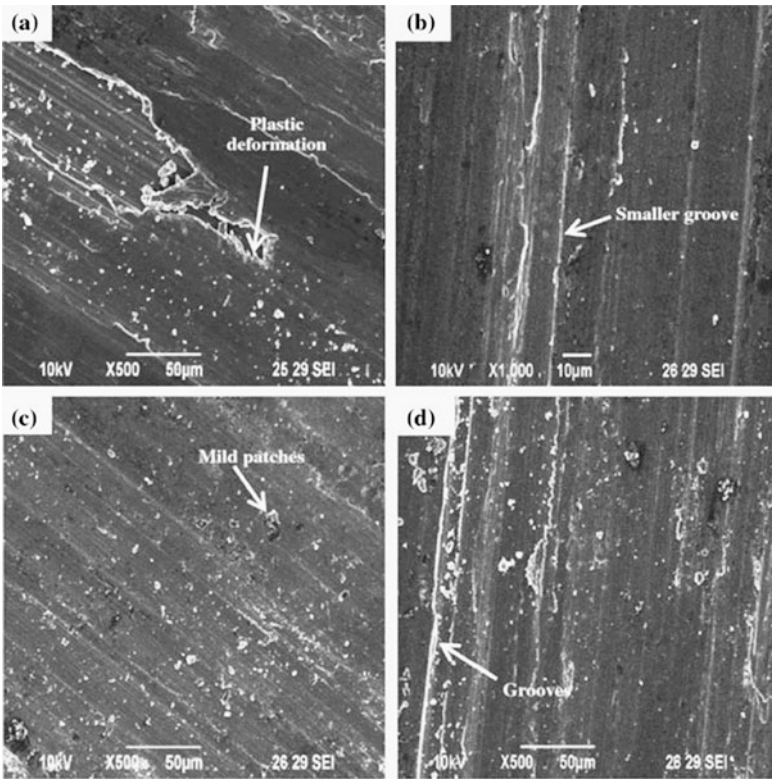

Fig. 2.10 Worn surfaces for an Al-Gr composites (**b**–**d**) with increasing Gr content, compared to the matrix alloy (**a**). Reprinted from [168], with permission from Elsevier

studies of these materials. Without information on transfer films, it makes it problematic to fully understand the third body flows and the mechanisms for replenishment of the graphitic tribofilm. Authors theorize that the replenishment comes from the subsurface of the composite, but tribofilms can also be replenished by recirculation flows between the counterface and wear track.

Similar trends in the appearance of the wear track morphology are also observed for CNT composites (see Fig. 2.11). As Zhou et al. [104] increased the CNT content in their composites, they observed a smoother wear surface. For only 5% CNT content, the wear track was rough and there was evidence of ploughed materials. For 10% and 20% addition of CNTs, the worn surface became smoother, with less evidence of ploughing. This was accompanied by reduction in friction and wear, as was presented above.

Carbon nanotubes can also be incorporated into a composite with cold spray methods. Bakshi et al. [89], using a composite powder, created Al-CNT composites and studied their tribology with a scratch tester. As can be seen in Fig. 2.12, the total wear volume of the scratch was decreased for all normal loads by the introduction of

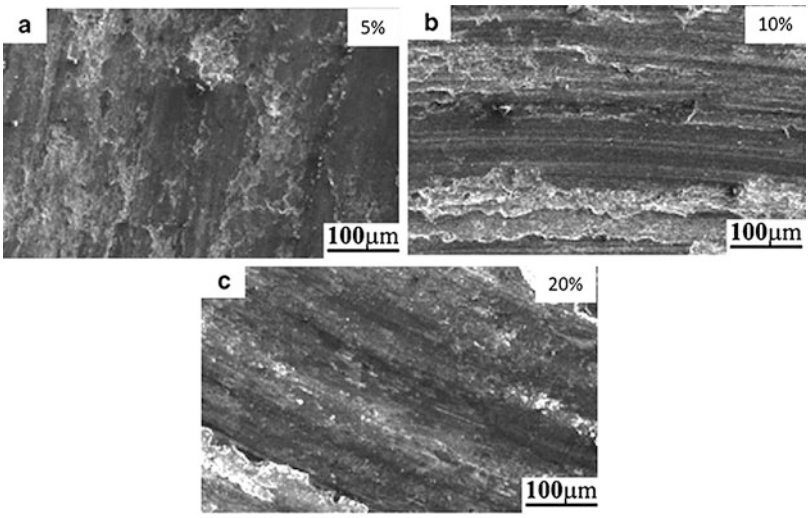

Fig. 2.11 Typical tribofilms observed for Al-CNT composites containing (**a**) 5%, (**b**) 10%, and (**c**) 20% CNTs made by powder metallurgy methods. Reprinted from [104], with permission from Elsevier

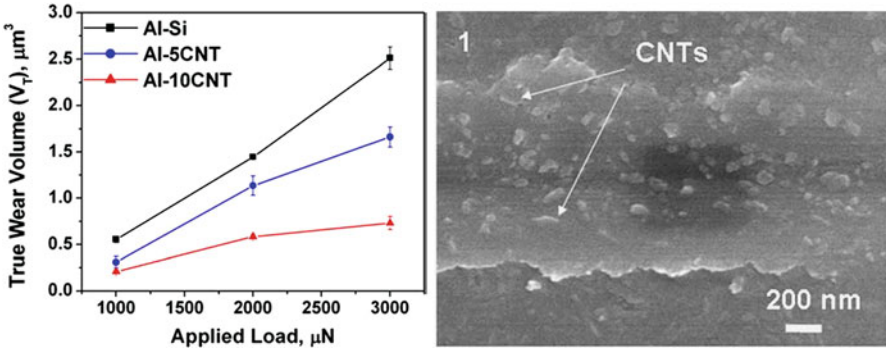

Fig. 2.12 Scratch testing wear results for an Al-CNT composite made by cold spray and corresponding observation of the worn surface with CNTs. Reprinted from [89], with permission from Elsevier

CNTs. The scratch track observed by SEM was found to have CNTs on the surface, which may have aided in the composite to resist wear during the scratch experiment.

Wear tracks can also be examined in cross sections, which can often give significant additional information on the exact nature of the material transformations in the tribofilms. These can be done as mechanical cross sections [169] but more recently can also be examined with focused ion beam (FIB) cross sectioning [98, 174, 175]. Figure 2.13 is an example of a mechanical cross-section of a wear track created on an Al alloy composite with 10% SiC and 4% Gr. In this study by Riahi

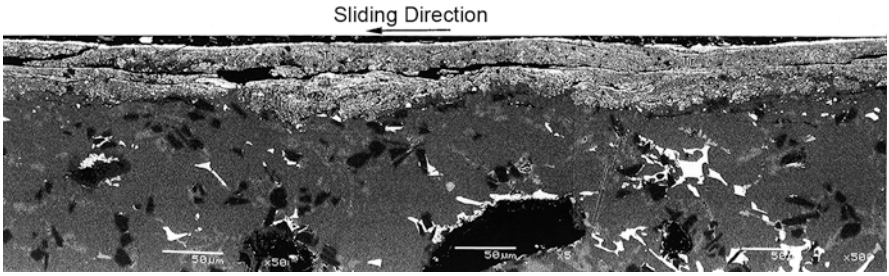

Fig. 2.13 Tribolayer observed on Al-10%SiC-5%Gr composite run against a steel-bearing material. The tribolayer in this case is primarily iron oxide with Al_3Ni and SiC particulates. Reprinted from [169], with permission from Elsevier

and Alpas [169], the composite was run in a block-on-ring test with a bearing steel, a tribo-test that more closely replicates the contact conditions the composite would encounter in service. Rather than high coverage of a carbonaceous tribofilm, the authors found that a thick tribofilm is formed that is composed of a mixture of iron and aluminum oxides, fractured SiC and intermetallic Ni_3Al, which is from the base alloy. Graphite did exist in these tribofilms, but clearly the mechanisms for lubrication and wear of this alloy are significantly more complicated than one can determine from observation of top-down wear track morphology, as was reviewed above.

Use of FIB microscopy in recent years allowed for high resolution observation of the cross section of worn surfaces and also provided the utility of being able to prepare TEM foils when desired. Use of these methods can better reveal the mechanisms for lubrication in SLMMCs. Figure 2.14 are cross sections prepared by FIB from a wear track on a Ni-3Ti-20C composite that was manufactured by laser additive manufacturing methods [98]. Each view is a region within the near surface of the wear track. Once can clearly observe an MML and distinct C tribofilm at the surface of all images. Also, striking is the observation of the mechanism of combined plastic deformation near surface and "wicking" of the carbon within the composite towards the surface to become part of the tribofilm. This observation is particularly interesting as the carbon can be brought to the surface without significant wear occurring but instead by simply the plastic deformation.

2.5 Metal-MoS_2, WS_2, h-BN, CaF_2, and BaF_2 SLMMCs

2.5.1 Tribological Behavior of SLMMCs Containing MoS_2, WS_2, h-BN, CaF_2, and BaF_2

Figures 2.15 and 2.16 summarized coefficient of friction observed in a number of different metal matrices of Cu, steel, Ni, and Ni-based alloy reinforced with MoS_2 and h-BN, respectively. The composites were fabricated by different manufacturing

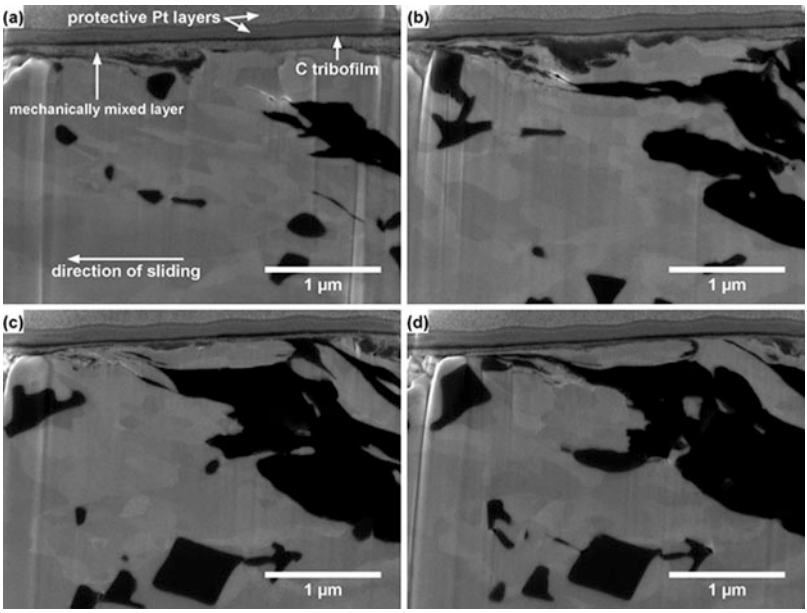

Fig. 2.14 Example of tribofilm formation in a Ni-3Ti-20C composite made by laser additive manufacturing methods. Reprinted from [98], with permission from Springer

methods such as powder metallurgy [34, 35, 122, 176], thermal spray [112, 142], cold spray [32], and laser cladding [132]. The tests were carried out with different tribometer configurations, mainly pin-on-disk and ball-on-plate, different normal loads, sliding speeds, and different counterface materials, e.g., different types of steels, Si_3N_4, alumina. Even though it is difficult to compare the absolute values due to the above variables, all the composites show some common trends. First of all, their coefficient of friction decreased with increasing solid lubricant content and then tended to keep constant or, in some cases, increased slightly. Early research carried out by Tsuya et al. demonstrated that in cold pressed Cu-MoS_2 composites, a minimum friction was reached at a MoS_2 concentration of 7–10% and remained fairly constant up to a concentration of close to 90% [179]. Similar trend was also observed in Gr reinforced SLMMCs by other researchers [64]. However, for the majority of the composites listed in Figs. 2.15 and 2.16, the lowest friction coefficient was around 0.4 or even higher. That is much higher than that sliding against blanket films of solid lubricants fabricated by physical vapor deposition and chemical vapor deposition, indicating metal matrix at the contact plays an important role. The effect of metal matrix component on friction coefficient has been analyzed theoretically by Rohatgi et al. [64]. The friction of an SLMMC can be written as

$$f = \left(1 - A_f\right) f_m + A_f f_f \tag{2.1}$$

Matrix	Cu	Cu	Ni-20Cr+W+Fe+C	Ni-20Cr+W+Al+Ti	316L
	◻	▷ ⬡	△ ○	▽	◁ ◇
Normal load (N)	5	40, 80	5	5	PV=1.1, 1.8
Sliding speed (m/s)	0.002	0.15	0.8	0.8	

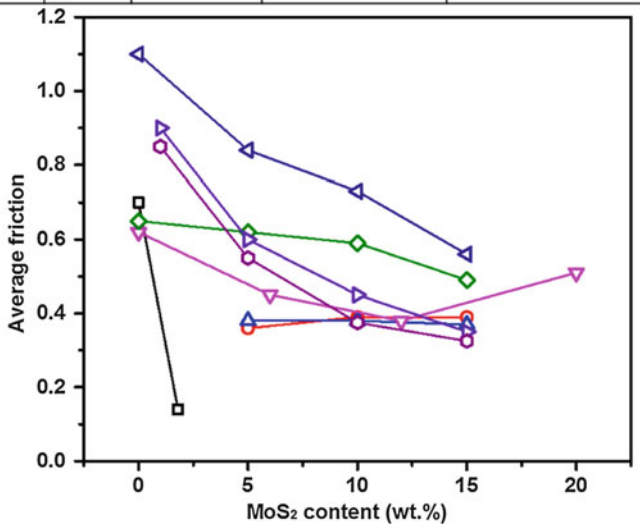

Fig. 2.15 Variation of average friction with content of MoS_2 for composites with different matrix materials and corresponding brief tribology testing parameters [32, 34, 35, 122, 176]

where A_f is fraction of lubricating tribofilm in the contact, f_f, f_m are friction coefficients of the lubricating tribofilm and matrix, respectively. Therefore, the coefficient of friction of composites may vary between f_m and f_f depending on solid lubricant content and ability of development and stability of lubricating film over sliding.

WS_2, BaF_2, and CaF_2 have been used as high temperature solid lubricants and incorporated with metals, e.g., Ni and Ni alloy using powder metallurgy techniques, plasma spray, and laser cladding. The coefficient of friction reduced significantly with even a small amount of solid lubricant in the composites, and this effect was even more pronounced at elevated temperatures [33, 114, 121, 135, 141]. The same trend was observed in wear rates. In general, BaF_2 and CaF_2 exhibit excellent wear resistance at a broad temperature range between room temperature and 1000 °C [112, 121], while WS_2 shows the lowest wear rate at 300 °C [33]. Strong matrix, combined with sulfides and fluorides, sometimes oxides formed at high temperature, are responsible for low friction and high wear resistance at high temperatures [121, 133]. It is worth to note that as the materials have to experience high temperature during fabrication, decomposition of solid lubricants are inevitable, even completely decomposed under some circumstances [114, 135]. However, some high temperature products, e.g., $CaCrO_4$ and $CaMoO_4$ (CaF_2 added

Matrix	Ni_3Al+Ag	Ni_3Al	Ni-20Cr+W+Mo+Al+Ti	Ni-20Cr+W+Mo+Al+Ti+Ag	NiCr+Cr_3C_2	Ni	Ni
	□	◇	△	▽	◁	○	▷
Normal load (N)	5	4.9	20	100	9.8	100	50
Sliding speed (m/s)	0.132	0.188	1	0.5	0.188	0.226	-

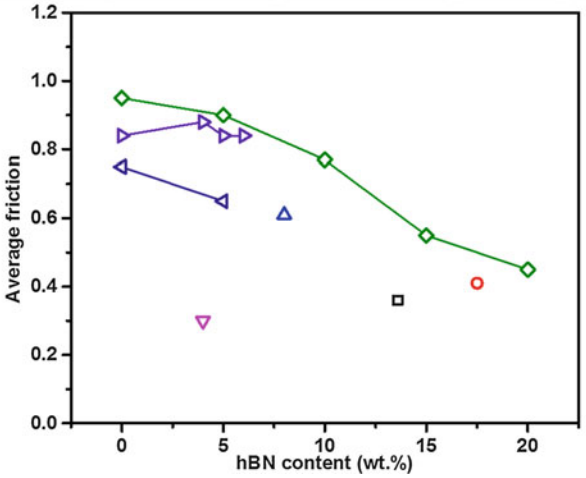

Fig. 2.16 Variation of average friction with content of h-BN for composites with different matrix materials and corresponding brief tribology testing parameters [109, 112, 118, 132, 142, 177, 178]

to Ni_3Al matrix), are lubricious and lead to improved tribological behavior at elevated temperatures [133].

Figure 2.17 shows wear rate evolution with solid lubricant content for composites with various matrix materials and fabricated by different manufacturing processes. Again, even though the absolute values cannot be compared because of different testing conditions and insufficient characterization on the composites, the general trends of wear rate with solid lubricant concentration are revealed. In Fig. 2.17a, the wear rates decreased more rapidly with increasing only a small amount of solid lubricants, and then tended to keep constant with further increase in MoS_2 or h-BN. However, as observed in the Gr SLMMCs, there was an opposite trend where wear rates increased with solid lubricant after a certain amount, as seen in Fig. 2.17b, c. Cold sprayed Cu-MoS_2 composites using admixed feedstock show continuous increase in wear track depth with increase in MoS_2 content (Fig. 2.17c right). The increase in wear rates was mainly due to degraded mechanical property induced by poor bonding strength between solid lubricant and metal matrix [32, 64, 116, 142]. In order to improve wear resistance, adding hard phase like ceramics to increase load-bearing capacity of the matrix was an effective method [3, 95, 130, 164]. Moreover, in the case of powder metallurgy route, increasing sintering temperature to get adequate bonding strength and low porosity was able to reduce significantly wear rate at higher h-BN content, as shown in Fig. 2.17b [126]. Post-plastic deformation, e.g., extrusion, was also able to decrease porosity effectively

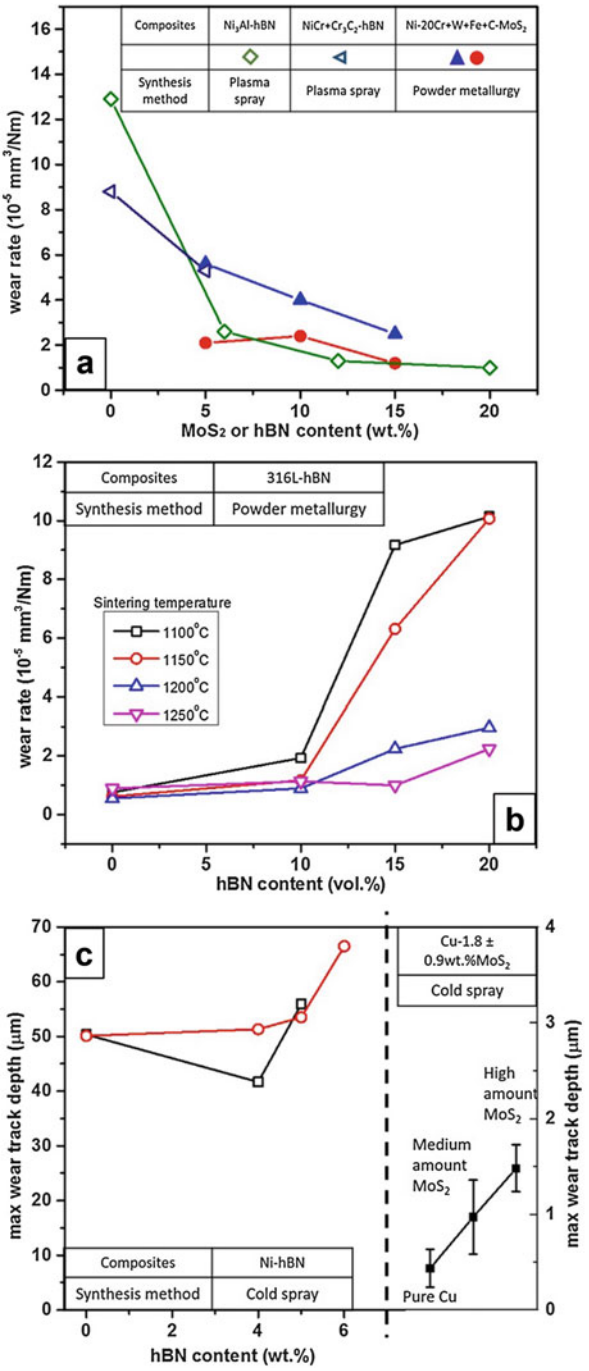

Fig. 2.17 Variation of wear rates with MoS_2 or h-BN content for composites with different metal matrix materials and various synthesis methods. (**a**) Wear rates of Ni alloys reinforced by MoS_2 or h-BN fabricated by plasma spray or powder metallurgy [35, 112, 142], (**b**) wear rates of 316L-h-BN composites developed using different sintering temperatures [125], and (**c**) wear rates of cold sprayed Ni-h-BN (left) [118] and Cu-MoS_2 (right) [32] composites

and therefore improve wear resistance [180]. As described in the Sect. 2.4.2, the transition point based on solid lubricant content above which wear rate starts climbing varies with manufacturing routes. In general, composites made by the liquid methods such as laser cladding and plasma spraying exhibit higher transition point than those fabricated by semisolid and solid methods, e.g., powder metallurgy and cold spray. As shown in Fig. 2.17a, c, plasma sprayed Ni_3Al-h-BN composites showed continuous decrease in wear rate up to 20 wt% h-BN, while for cold sprayed Ni-h-BN composites, wear rate started increasing at around 5 wt% h-BN.

Except for materials, there are some testing parameters that affect wear rate evolution and they are normal load and sliding speed. The influence of those two factors on friction and wear of SLMMCs have been studied extensively and well summarized by Omrani et al. and Rohatgi et al. [4, 5, 64, 181].

2.5.2 Third Bodies Observed for SLMMCs Containing MoS_2, WS_2, h-BN, CaF_2, and BaF_2

As described in Sect. 2.2.1, friction and wear mechanisms are conventionally examined by observation of sliding contact, i.e., worn surfaces using ex situ methods. Even though the design of SLMMCs, as shown in Fig. 2.1, is to form a full solid lubricating film on the wear track or contact, the role of metal matrix has to be taken into account. In general, for metal-metal contact, incorporation of solid lubricants reduced adhesive wear to some extent depending on the solid lubricant concentration and the testing condition [34, 122]. For Cu-MoS_2 composites sliding against Cu, powdery particles of solid lubricant, not a full film, in the contact were responsible for reduced friction and adhesion and was the main wear mechanism [122]. Mahathanabodee et al. [36, 125] proposed a wear model for a 316L-h-BN and a 316L-h-BN-MoS_2 composites sliding against high-chromium steel counterfaces. They observed adhesive wear, abrasive wear, oxidation, formation of a compact layer, as well as delamination. The compact layer consisting of metal, sulfides, h-BN, and oxide helped to reduce friction and wear. However, this layer tended to be detached and caused delamination due to cyclic loading over sliding. WS_2 is used as a high temperature solid lubricant, and the mechanism of improving tribological behavior is presented in Fig. 2.18 [33]. Without WS_2, large pits were found at 300 °C wear track, therefore abrasive and adhesive wear played a role. However, for NiCr/Cr_3C_2/WS_2 coating, WS_2 and newly formed CrS generated transfer films in the contact, leading to a smoother wear track and lower friction coefficient. Moreover, as degradation of mechanical property at 300 °C was minor due to presence of Cr_7C_3, laser clad NiCr/Cr_3C_2/WS_2 composite coating exhibited a good combination of friction and wear at 300 °C. In addition, ceramic phase additives alter wear mechanism of self-lubricating composites as well. Xu et al. [130] reported adhesion, delamination, and plastic deformation were the main wear mechanisms in a Ni-MoS_2 composite, while incorporation of TiC helped to generate a smoother worn surface and eliminated adhesive wear. Although wear mechanisms seem to be identified

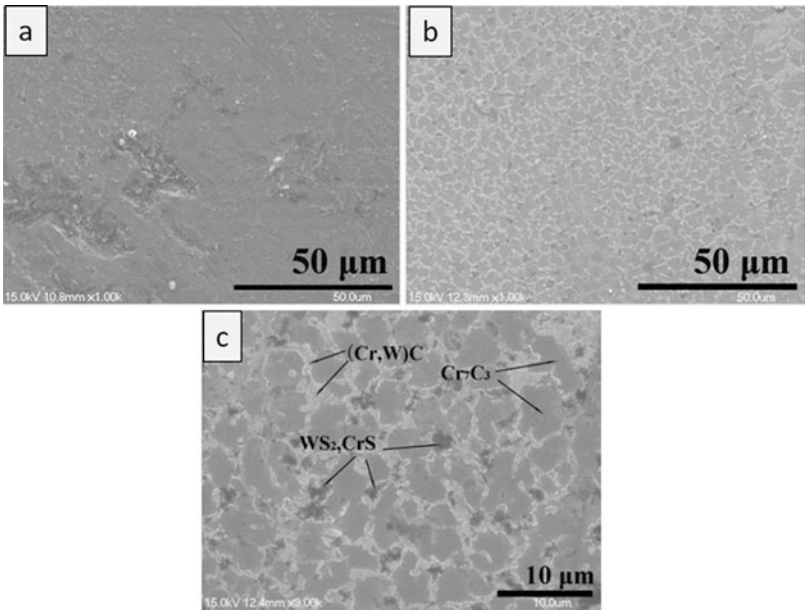

Fig. 2.18 Wear tracks of (**a**) laser clad NiCr/Cr_3C_2 coating and (**b**, **c**) laser clad NiCr/Cr_3C_2/WS_2 coating at 300 °C. Reprinted from [33], with permission from Elsevier

through observation of worn surfaces by ex situ approach, more detailed information on dynamics of third bodies in the contact, e.g., initiation of tribofilms and transfer films, as well as their evolution, is helpful to better understand friction and wear behavior. That is the design purpose of in situ tribometry, as discussed in the Sect. 2.2.1. A combination of ex situ and in situ method has been applied on cold sprayed Cu-MoS_2 composites, and the results will be presented in the remainder of this section.

Zhang et al. [32] reported recently that when Cu-1.8 wt% MoS_2 composite rubbing against alumina, how MoS_2 smeared out forming discontinuous tribofilms, and their evolution with sliding. Spatial friction was extracted to link local coverage of MoS_2 tribofilms. As shown in Fig. 2.19, at 100 cycles, MoS_2 was smeared out and formed MoS_2-rich patches in the wear track. The local friction distribution combined with chemical analysis demonstrated that higher MoS_2 content zones generated lower local friction. The MoS_2 patches were expanded and tended to distribute more homogenously as sliding continued (see MoS_2 distribution of the 1000 cycle wear track in Fig. 2.20). Inside the patches, MoS_2 was found to be powdery and mixed with Cu_2O and/or Cu (Figs. 2.19d, 2.20d, and 2.21e). The mechanism for low friction in a metal-MoS_2 composite was expected to be different from that found in blanket films of MoS_2 made by physical vapor deposition (PVD) or similar methods, which was discussed in Sect. 2.2.2 [59, 182, 183]. The main feature of these latter coatings was to form transfer films on the counterfaces, which led to MoS_2 sliding versus MoS_2 and friction coefficients in the range of 0.02–0.06

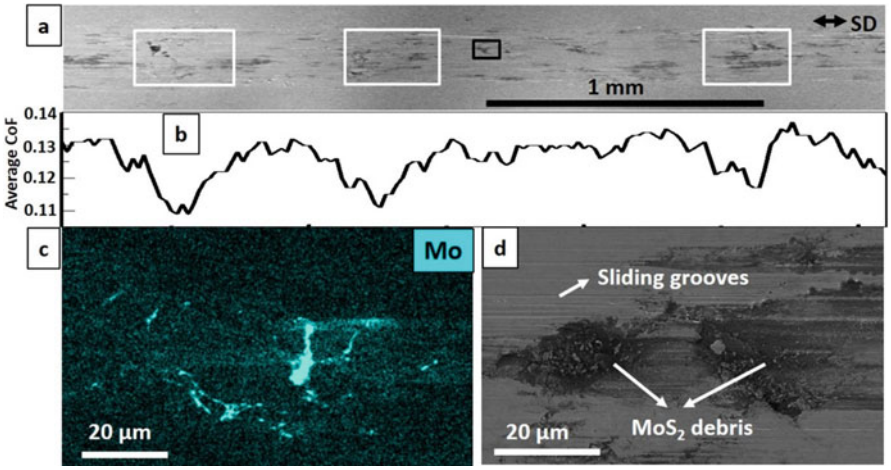

Fig. 2.19 Top-down view of the Cu-MoS_2 wear track after a 100 cycle test. (**a**) Overall morphology; (**b**) spatial friction along the wear track at the 100th cycle; (**c**) an EDX map of the black rectangle in (**a**); (**d**) a closer view of the wear track morphology. Reprinted from [32], with permission from Springer

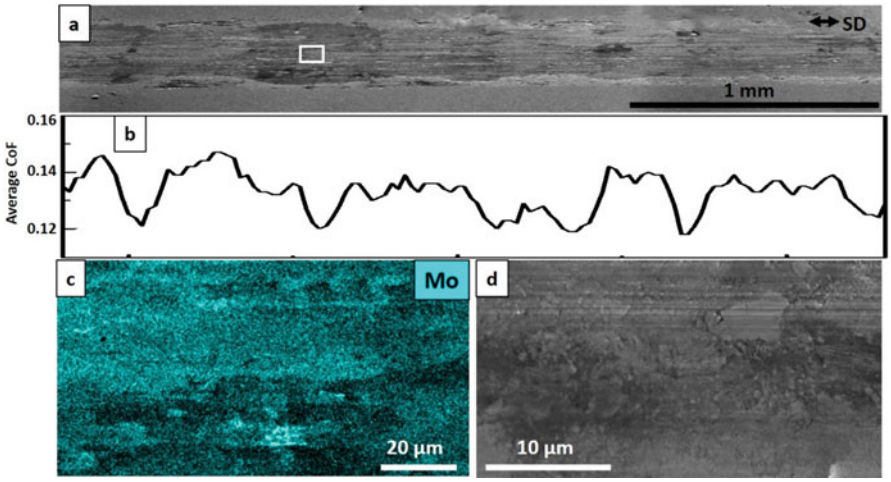

Fig. 2.20 Top-down view of the Cu-MoS_2 wear track after a 1000 cycle test. (**a**) Overall morphology; (**b**) spatial friction along the wear track at the 100th cycle; (**c**) an EDX map of the black rectangle in (**a**); (**d**) a closer view of the wear track morphology. Reprinted from [32], with permission from Springer

in dry air at similar test conditions to those performed here [59]. Thus, while there is a significant friction reduction due to the presence of MoS_2, the mechanisms for this reduction were modified due to the presence of the Cu. The first noticeable difference was the lack of a transfer film observed at 100 and 1000 cycle tests (Fig. 2.21a, b).

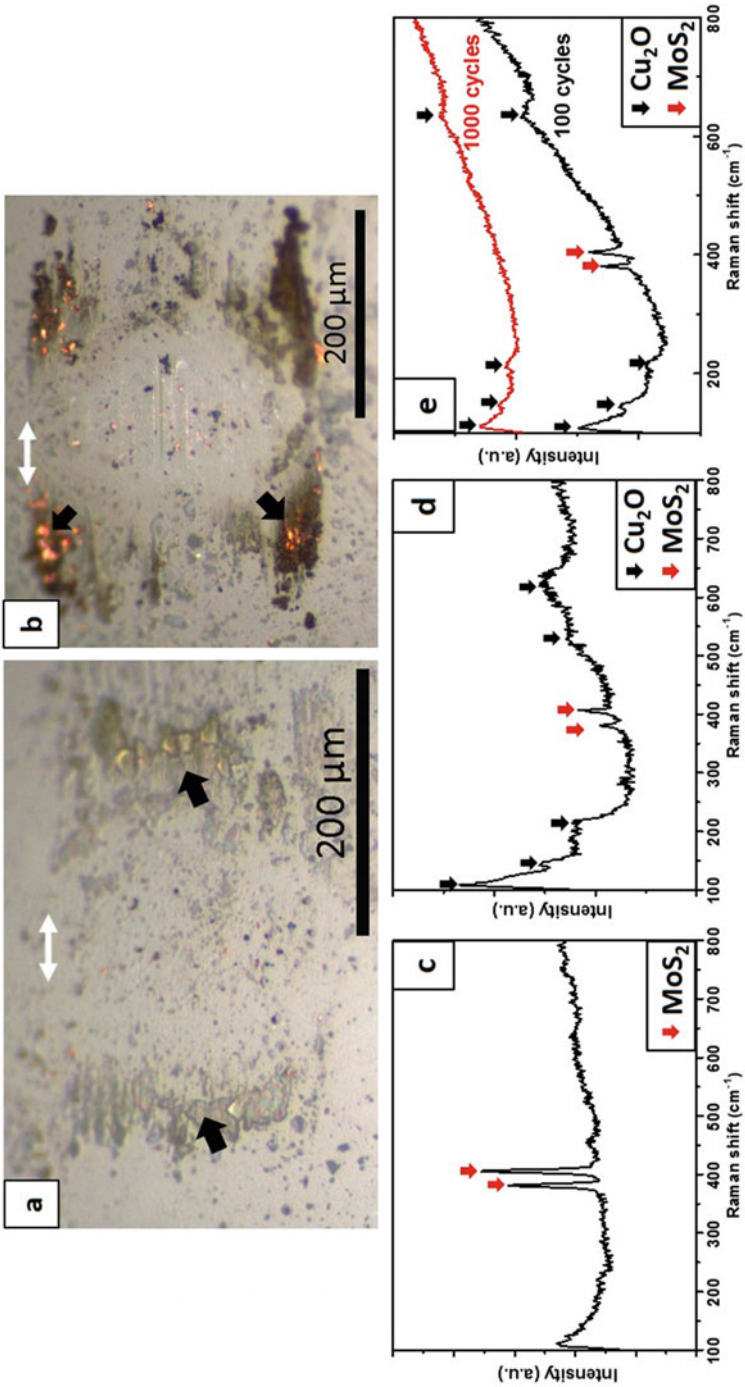

Fig. 2.21 Micrographs of the counterfaces mating with the Cu-MoS_2 coating after (**a**) 100 cycles and (**b**) 1000 cycles. Transferred patches and/or debris were found outside the contact, indicated as black arrows. Their Raman spectra were shown in (**c**) and (**d**), respectively. (**e**) Raman spectra taken from the wear tracks. White arrows indicate sliding direction. Reprinted from [32], with permission from Springer

With only 1.8 wt% MoS_2 in the coating, any transfer films that did form were readily removed and redeposited onto the wear track. This was due to the interactions of MoS_2 with the wear track, which was primarily Cu – a very different contact condition compared to sliding on a PVD coating with a constant source of MoS_2. With the interactions of the metal, the transfer films were unstable and continuously removed, ultimately resulting in MoS_2 patches on the wear track that were expanded over sliding (Figs. 2.19d and 2.20d).

The VAM within MoS_2-rich tribofilms was also explored briefly in this study [32]. Using the two-term friction model that is commonly employed to combine two velocity accommodation modes with an assumption that interaction between the friction mechanisms is negligible [39], the total friction can be written as

$$\mu = \mu_{int} + \mu_{fracture} \tag{2.2}$$

where μ_{int} is friction from interfacial sliding and $\mu_{fracture}$ is the friction from fracture. Dvorak et al. [8, 56, 57] proposed a similar model for taking account of two friction mechanisms in MoS_2. For Cu-1.8 wt% MoS_2, the low MoS_2 content in the coating and the absence of a persistent MoS_2 transfer film on the counterface indicate that interfacial sliding between MoS_2 and MoS_2 did not occur to any great extent. The process by which the transfer films were removed and deposited back to the wear track as powdery MoS_2 was primarily related to the fracture of MoS_2. So the velocity difference was mostly accommodated by fracturing of MoS_2 third bodies. Therefore, $\mu_{int} \cong 0$, and $\mu \cong \mu_{fracture}$. Uemura et al. [184] demonstrated that fracture dominated friction was three to four times higher than interfacial sliding (i.e., $\mu_{fracture} \cong 3.5*\mu_{int}$). Also, Dvorak et al. [8, 56, 57] showed that the friction induced by interfacial sliding in dry air (i.e., $\mu \cong \mu_{int}$) under a wide range of contact pressure (0.41–1.39 GPa) was below 0.05. Thus, based on the results of Uemura and Dvorak, an estimate of fracture-induced friction indicated it should be roughly 0.18 or below. This estimate was in a good agreement with the present study, where the friction of the high MoS_2 zones was 0.11–0.12. This analysis helped to understand how low friction can be observed with MoS_2 through a primarily fracture-based process instead of interfacial shearing. However, the elevated friction compared to an interfacial sliding mechanism must also partly be due to the occurrence of some metallic friction, evidenced by sliding grooves at the zones with little/no MoS_2 (Fig. 2.19d) and oxidation (Fig. 2.21e).

Cross-sectional microstructures of the wear tracks exhibit influence of solid lubricants on tribologically modified microstructure and therefore permit a better understanding of tribological behavior of SLMMCs. As shown in Fig. 2.22, in the Cu-MoS_2 wear track, sliding induced a cohesive mechanically mixed layer (MML) with fine cracks and a shallow dynamic recrystallized (DRX) layer 3–5 μm deep, where a decrease in defect density was observed but no significant grain growth. However, for the Cu wear track, sliding introduced large cracks within the MML. The DRX layer penetrated into the coating as deep as 10–30 μm and substantial grain growth was found in the DRX layer. The minor changes in subsurface microstructure and phase transformation in the Cu-MoS_2 wear track compared to Cu wear track

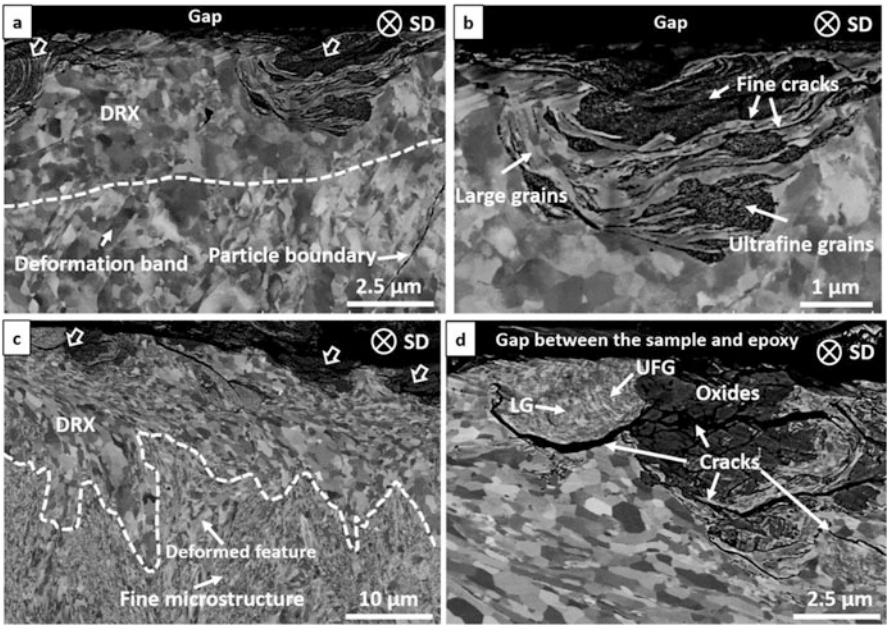

Fig. 2.22 (**a**) Micrograph of cross section of the Cu-MoS_2 wear track after a 3000 cycle test. The hollow arrows denote MML, and the dashed line the border of the sliding-induced microstructure and as-sprayed microstructure. (**b**) A closer view of the sliding-induced microstructure. (**c**) Micrograph of cross section of the Cu wear track after a 3000 cycle test. The hollow arrows denote MML, the dashed line the border of the sliding-induced microstructure and the as-sprayed microstructure. (**d**) A closer view of the sliding-induced microstructure. SD indicates sliding direction. Reprinted from [32], with permission from Springer

probably resulted from a much minder stress field generated underneath the Cu-MoS_2 wear tracks [32, 185–187]. There is a chance that frictional heating might play a role on the microstructural modification [188].

As discussed in Sect. 2.2.1, for SLMMCs, even though traditional ex situ techniques have been used extensively to observe third body behaviors, e.g., formation and evolution of lubricating tribofilms and transfer films, the effectiveness of replenishment process and the mechanisms have not been fully understood. In situ tribology technique is capable of capturing third body "processes" over the whole testing, which provides generation and dynamics of lubricating films at the contact. Here we present formation of MoS_2 tribofilms and transfer films at the very beginning and how they were depleted with sliding. More details on in situ tribometer setup can be found in [16] and sliding wear testing parameters in [32]. As shown in Fig. 2.23, once sliding commenced, patchy MoS_2 transfer film was formed. Where and how much of the transfer film can be generated largely depent on local MoS_2 content. The transfer films were then deposited onto the wear track when rubbing against pure Cu, and were consumed completely eventually, as shown in Fig. 2.23b–d. This process continued with sliding. At 20 cycles (see Fig. 2.24a),

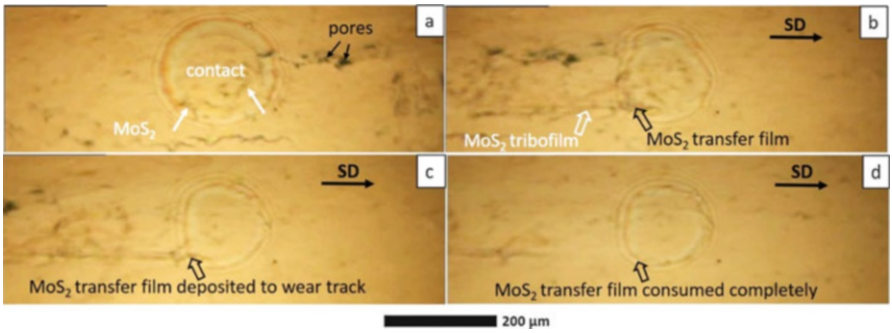

Fig. 2.23 In situ micrographs of Cu-MoS_2 composite during the first half cycle. (**a**) Right before sliding, followed by (**b**–**d**) where sliding commenced. SD indicates sliding direction. (Mining and Materials Engineering, McGill University, Montreal, Canada)

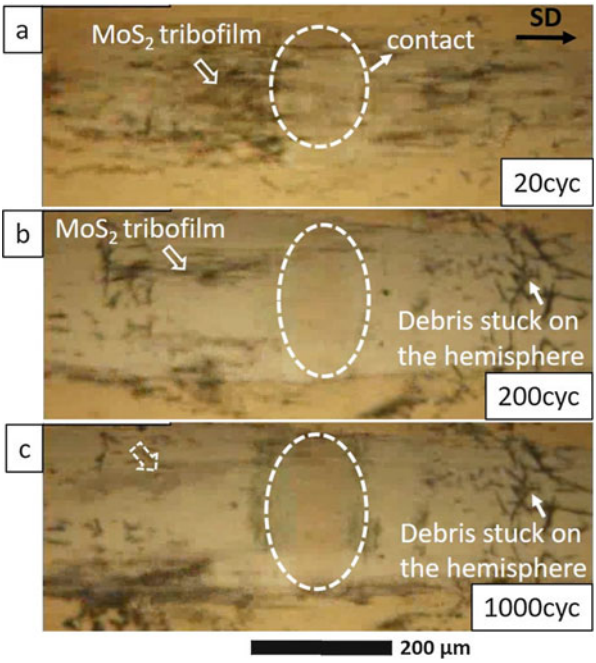

Fig. 2.24 In situ micrographs of Cu-MoS_2 composite at (**a**) 20 cycles, (**b**) 200 cycles, and (**c**) 1000 cycles. The same spot was taken to investigate evolution of the lubricating film. Dashed lines of ellipses indicate contact, while the arrow with dashed lines denotes the MoS_2 tribofilm become barely visible through optical microscope. (Mining and Materials Engineering, McGill University, Montreal, Canada)

more MoS_2 tribofilms were developed, indicating MoS_2 was expanded more extensively and in the meantime MoS_2 was replenished as wearing through the top surface. The MoS_2 tribofilms were then depleted gradually as seen in Fig. 2.24b, c. They could become wear debris deposited onto the counterface or outside the wear track. It is worth noting that even though only a few visible patchy MoS_2 tribofilms over the majority of sliding, the presence of MoS_2 eliminated metal oxidation comparing to the pure Cu case (not shown). These results are consistent with wear

track morphology observation by ex situ techniques (Fig. 2.22). Even though higher resolution micrographs and in situ chemical/phase composition analysis, e.g., in situ Raman spectroscopy, are required to better understand third body generation and evolution over sliding, we believe combination of ex situ and in situ methods are able to reveal third body behavior of SLMMCs more comprehensively.

2.6 Applications, Challenges, and Future Directions

SLMMCs remain an important class of engineering materials, especially considering global initiatives for green manufacturing and increased sustainability in engineering design. These materials find applications in aerospace, automotive, marine, and other sectors where tribological contacts are made that require low friction, such as bearings, bushings, and piston liners. Many different metal matrices have been studied (e.g., Cu, Mg, Al, Ni, Ti, and their alloys) with a range of solid lubricants (e.g., Gr, CNTs, G, MoS_2, WS_2, h-BN, and others). One also finds SLMMCs manufactured by a wide range of methods that have been reviewed here, from the mature stir casting method for Al alloys with Gr to the more recent techniques of cold spray, friction stir processing, and laser additive manufacturing methods. Thus, there is a significant body of scientific literature and knowledge base for SLMMCs. However, based on this review, we have identified some areas of future research that could make significant impact on understanding of the lubrication mechanisms for SLMMCs and also the development of SLMMCs with optimized properties.

The basic understanding of the lubrication mechanisms of SLMMCs consists of tribofilm formation, which is the formation of a surface layer that consists of lubricating material that reduce the fraction of metal-to-metal junctions in the sliding contact. However, as shown in this review the structure of a tribofilm can be considerably more complex than this. In the work of Riahi and Alpas [169], they observed a tribofilm that was composed of many components with a small fraction of the graphite lubricant. Researchers should devote more efforts on describing the exact nature of the tribofilms for SLMMCs as their formation is key for the function of the composite, but the mechanism and the nature of their formation are not always fully elucidated.

Generally, third body flows and lubrication mechanisms for SLMMCs deviate significantly from blanket films of solid lubricants. For blanket films, there is a large volume fraction of solid lubricant available; the VAM is solid lubricant vs. solid lubricant or interfacial shearing of the solid lubricant, as depicted in Fig. 2.2. For SLMMCs, the total volume fraction of lubricant is lower. Often one finds that transfer films do not persist in the sliding contact, as was shown by in situ tribometry above in the work of Zhang et al. (McGill University). Any transfer film material formed generally flows back to the wear track in recirculation flow or out of the contact as debris. This means the mechanisms observed by Mogonye et al. [98] are more important. An understanding of the replenishment mechanisms for the tribofilms from the near surface solid lubricant particles would be key in better design of SLMMCs. The flow of solid lubricant materials toward the surface can naturally occur by wear or

by plastic deformation, but the process must have a dependence on the fabrication methods of the composite, lubricant content and morphology, and the microstructure of the matrix itself. Researchers have already described these as being key variables for the performance of the composites, but these links are not as strong as they could be without more detailed information on the mechanisms of near surface lubricant flow, tribofilm formation and structure, and the recirculation flow of lubricants.

SLMMCs have an opportunity to undergo a significant revolution in both materials and processing/manufacturing. In terms of materials, researchers are actively exploring incorporation of newer forms, often nanostructured, of popular lubricants. Recent excitement on graphene and before that CNTs have translated to their use in SLMMCs. Similarly, 2D versions of MoS_2 are becoming readily available and can be utilized for making SLMMCs. Challenges of course remain for these materials. Researchers must focus as best they can on side-by-side comparisons [76] between these newer materials and traditional forms of the lubricants. Otherwise, the understanding of performance differences becomes lost in the cloud of tribological test parameters. Also, it is critical that the lubricants be examined with electron microscopy and other spectroscopic methods to quantify the state of the lubricant in the SLMMC postprocessing.

On the manufacturing side, new processing routes provide new possibilities for SLMMCs. In particular additive manufacturing provides a new vista. While most additive manufacturing researchers are focused on making bulk parts from metals and alloys, there is a real possibility for using these techniques to tailor the properties for SLMMCs, including but not limited to a more precise control of the lubricant content and morphology in the composite. However, many of these techniques are laser based, and challenges on control of lubricant state in the composite would be a key issue. Similarly, cold spray, which is currently a method primarily focused on metals and coatings, has the potential to become an additive manufacturing method utilized for SLMMCs. Even though cold spray eliminates or avoids decomposition of the solid lubricants that is inevitable for most of the other manufacturing processes, challenges for this technique are precise control of powder delivery systems and development of optimized feedstocks that are suitable for cold spray. The feedstocks can be conceivably modified to composite powders using dryer spraying technique, metal-coated solid lubricant powders made by deposition or ball milling, and even combination of them, i.e., metal-coated composite powders. These pretreatments could improve cold sprayability of the materials according to deposition mechanism described in Sect. 2.3.5. Moreover, due to poor sprayability of solid lubricants, in situ formation of solid lubricants during post spraying treatment, e.g., heat treatment, could avoid spraying solid lubricant directly. This could promote a new route to fabricate SLMMCs using cold spray. In addition, several alternatives of conventional lamellar solid lubricants are some oxides, e.g., TiO_2, and soft metals, e.g., Sn, which could be used as solid lubricants at elevated temperature. In fact, TiO_2 ceramic coating has been sprayed by high pressure cold spray system and low pressure cold spray system [189, 190]. Even though there are some challenges, cold spray provides an interesting opportunity to develop a next generation of SLMMCs.

References

1. Daniel, I.M., Ishai, O.: Engineering Mechanics of Composite Materials. Oxford University Press, New York (1994)
2. Prasad, S., Asthana, R.: Aluminum metal-matrix composites for automotive applications: tribological considerations. Tribol. Lett. **17**(3), 445–453 (2004)
3. Miracle, D.B.: Metal matrix composites – from science to technological significance. Compos. Sci. Technol. **65**(15–16), 2526–2540 (2005)
4. Omrani, E., et al.: Influences of graphite reinforcement on the tribological properties of self-lubricating aluminum matrix composites for green tribology, sustainability, and energy efficiency – a review. Int. J. Adv. Manuf. Technol. **83**(1–4), 325–346 (2016)
5. Omrani, E., et al.: New emerging self-lubricating metal matrix composites for tribological applications. In: Davim, P.J. (ed.) Ecotribology: Research Developments, pp. 63–103. Springer International Publishing, Cham (2016)
6. Dellacorte, C., Fellenstein, J.A.: The effect of compositional tailoring on the thermal expansion and tribological properties of PS300: a solid lubricant composite coating. Tribol. Trans. **40**(4), 639–642 (1997)
7. Zhang, X., et al.: Carbon nanotube-MoS_2 composites as solid lubricants. ACS Appl. Mater. Interfaces. **1**(3), 735–739 (2009)
8. Chromik, R.R., et al.: In situ tribometry of solid lubricant nanocomposite coatings. Wear. **262** (9–10), 1239–1252 (2007)
9. Godet, M.: The third-body approach: a mechanical view of wear. Wear. **100**(1), 437–452 (1984)
10. Godet, M.: Third-bodies in tribology. Wear. **136**(1), 29–45 (1990)
11. Rigney, D.A., Karthikeyan, S.: The evolution of tribomaterial during sliding: a brief introduction. Tribol. Lett. **39**(1), 3–7 (2010)
12. Biswas, S.K.: Wear of metals: a material approach. In: Stachowiak, G.W. (ed.) Wear: Materials, Mechanisms and Practice, pp. 21–36. Wiley, West Sussex (2005)
13. Descartes, S., Busquet, M., Berthier, Y.: An attempt to produce ex situ TTS to understand their mechanical formation conditions – the case of an ultra high purity iron. Wear. **271**(9–10), 1833–1841 (2011)
14. Tumbajoy-Spinel, D., et al.: Assessment of mechanical property gradients after impact-based surface treatment: application to pure α-iron. Mater. Sci. Eng. A. **667**, 189–198 (2016)
15. Singer, I.L.: Solid lubrication processes. In: Singer, I.L., Pollock, H.M. (eds.) Fundamentals of Friction, pp. 237–261. Kluwer, Dordrecht (1992)
16. Chromik, R., Strauss, H., Scharf, T.: Materials phenomena revealed by in situ tribometry. JOM. **64**(1), 35–43 (2012)
17. Wahl, K.J., Sawyer, W.G.: Observing interfacial sliding processes in solid – solid contacts. MRS Bull. **33**(12), 1159–1167 (2008)
18. Berthier, Y., Godet, M., Brendle, M.: Velocity accommodation in friction. Tribol. Trans. **32**(4), 490–496 (1989)
19. Scharf, T.W., Singer, I.L.: Role of third bodies in friction behavior of diamond-like nanocomposite coatings studied by in situ tribometry. Tribol. Trans. **45**(3), 363–371 (2002)
20. Scharf, T.W., Singer, I.L.: Quantification of the thickness of carbon transfer films using Raman tribometry. Tribol. Lett. **14**, 137–146 (2003)
21. Scharf, T.W., Singer, I.L.: Monitoring transfer films and friction instabilities with in situ Raman tribometry. Tribol. Lett. **14**, 3–8 (2003)
22. Scharf, T.W., Singer, I.L.: Role of the transfer film on the friction and wear of metal carbide reinforced amorphous carbon coatings during run-in. Tribol. Lett. **36**(1), 43–53 (2009)
23. Strauss, H.W., et al.: In situ tribology of nanocomposite Ti-Si-C-H coatings prepared by PE-CVD. Wear. **272**, 133–148 (2011)
24. Wahl, K.J., Chromik, R.R., Lee, G.Y.: Quantitative in situ measurement of transfer film thickness by a Newton's rings method. Wear. **264**(7–8), 731–736 (2008)

25. Shockley, J.M., et al.: The influence of Al_2O_3 particle morphology on the coating formation and dry sliding wear behavior of cold sprayed Al-Al_2O_3 composites. Surf. Coat. Technol. **270**, 324–333 (2015)
26. Sriraman, K.R., et al.: Tribological behavior of electrodeposited Zn, Zn-Ni, Cd and Cd-Ti coatings on low carbon steel substrates. Tribol. Int. **56**, 107–120 (2012)
27. Stoyanov, P., et al.: Combining in situ and online approaches to monitor interfacial processes in lubricated sliding contacts. MRS Commun. 6(3), 301–308 (2016)
28. Shockley, J.M., et al.: Third body behavior during dry sliding of cold-sprayed Al-Al_2O_3 composites: in situ tribometry and microanalysis. Tribol. Lett. **54**(2), 191–206 (2014)
29. Shockley, J.M., et al.: In situ tribometry of cold-sprayed Al-Al_2O_3 composite coatings. Surf. Coat. Technol. **215**, 350–356 (2013)
30. Berthier, Y.: Experimental evidence for friction and wear modelling. Wear. **139**(1), 77–92 (1990)
31. Alidokht, S.A., et al.: Role of third-bodies in friction and wear of cold-sprayed Ti and Ti-TiC composite coatings. Tribol. Lett. 65, 114 (2017)
32. Zhang, Y., et al.: Tribological behavior of a cold-sprayed Cu–MoS_2 composite coating during dry sliding wear. Tribol. Lett. **62**(1), 1–12 (2016)
33. Yang, M.-S., et al.: Microstructure and wear behaviors of laser clad NiCr/Cr_3C_2–WS_2 high temperature self-lubricating wear-resistant composite coating. Appl. Surf. Sci. **258**(8), 3757–3762 (2012)
34. Raadnui, S., Mahathanabodee, S., Tongsri, R.: Tribological behaviour of sintered 316L stainless steel impregnated with MoS_2 plain bearing. Wear. **265**(3), 546–553 (2008)
35. Li, J.L., Xiong, D.S.: Tribological properties of nickel-based self-lubricating composite at elevated temperature and counterface material selection. Wear. **265**(3), 533–539 (2008)
36. Mahathanabodee, S., et al.: Dry sliding wear behavior of SS316L composites containing h-BN and MoS_2 solid lubricants. Wear. **316**(1), 37–48 (2014)
37. Scharf, T.W.: Low friction coatings. In: Bruce, R. (ed.) Handbook of Lubrication and Tribology. CRC Press, Boca Raton (2012)
38. Scharf, T.W., Prasad, S.V.: Solid lubricants: a review. J. Mater. Sci. **48**(2), 511–531 (2012)
39. Bowden, F.P., Tabor, D.: The Friction and Lubrication of Solids, vol. 1. Oxford University Press, New York (2001)
40. Erdemir, A., Fontaine, J., Donnet, C.: An overview of superlubricity in diamond-like carbon films. In: Donnet, C., Erdemir, A. (eds.) Tribology of Diamond-Like Carbon Films: Fundamentals and Applications, pp. 237–262. Springer US, Boston (2008)
41. Fontaine, J., Donnet, C., Erdemir, A.: Fundamentals of the tribology of DLC coatings. In: Donnet, C., Erdemir, A. (eds.) Tribology of Diamond-Like Carbon Films: Fundamentals and Applications, pp. 139–154. Springer US, Boston (2008)
42. Hoffman, E.E., Marks, L.D.: Graphitic carbon films across systems. Tribol. Lett. **63**(3), 32 (2016)
43. Liu, Y., Erdemir, A., Meletis, E.I.: An investigation of the relationship between graphitization and frictional behavior of DLC coatings. Surf. Coat. Technol. **86**, 564–568 (1996)
44. Liu, Y., Erdemir, A., Meletis, E.I.: A study of the wear mechanism of diamond-like carbon films. Surf. Coat. Technol. **82**(1), 48–56 (1996)
45. Fontaine, J., et al.: Tribological behaviour of metal-DLC nanocomposite coatings: the critical role of tribofilm build-up. In: World Tribology Congress 2009 – Proceedings (Kyoto, Japan) (2009)
46. Pastewka, L., Moser, S., Moseler, M.: Atomistic insights into the running-in, lubrication, and failure of hydrogenated diamond-like carbon coatings. Tribol. Lett. **39**(1), 49–61 (2010)
47. Al-Azizi, A.A., et al.: Surface structure of hydrogenated diamond-like carbon: origin of run-in behavior prior to superlubricious interfacial shear. Langmuir. **31**(5), 1711–1721 (2015)
48. Berman, D., et al.: Macroscale superlubricity enabled by graphene nanoscroll formation. Science. **348**(6239), 1118–1122 (2015)
49. Berman, D., et al.: Nanoscale friction properties of graphene and graphene oxide. Diam. Relat. Mater. **54**(1), 91–96 (2015)

50. Berman, D., et al.: Extraordinary macroscale wear resistance of one atom thick graphene layer. Adv. Funct. Mater. **24**(42), 6640–6646 (2014)
51. Berman, D., Erdemir, A., Sumant, A.V.: Few layer graphene to reduce wear and friction on sliding steel surfaces. Carbon. **54**, 454–459 (2013)
52. Spalvins, T.: Lubrication with sputtered MoS_2 films: principles, operation, and limitations. J. Mater. Eng. Perform. **1**(3), 347–351 (1992)
53. McDevitt, N.T., Donley, M.S., Zabinski, J.S.: Utilization of Raman spectroscopy in tribochemistry studies. Wear. **166**(1), 65–72 (1993)
54. Liang, T., et al.: First-principles determination of static potential energy surfaces for atomic friction in MoS_2 and MoO_3. Phys. Rev. B Condens. Matter Mater. Phys. **77**(10), 104105 (2008)
55. Liang, T., et al.: Energetics of oxidation in MoS_2 nanoparticles by density functional theory. J. Phys. Chem. C. **115**(21), 10606–10616 (2011)
56. Dvorak, S.D., Wahl, K.J., Singer, I.L.: In situ analysis of third body contributions to sliding friction of a Pb-Mo-S coating in dry and humid air. Tribol. Lett. **28**(3), 263–274 (2007)
57. Wahl, K.J., Belin, M., Singer, I.L.: A triboscopic investigation of the wear and friction of MoS_2 in a reciprocating sliding contact. Wear. **214**(2), 212–220 (1998)
58. Hoffman, E.E., Marks, L.D.: Soft interface fracture transfer in nanoscale MoS_2. Tribol. Lett. **64**(1), 1 (2016)
59. Wahl, K.J., Singer, I.L.: Quantification of a lubricant transfer process that enhances the sliding life of a MoS_2 coating. Tribol. Lett. **1**(1), 59–66 (1995)
60. Lince, J.R., et al.: Tribochemistry of MoS_3 nanoparticle coatings. Tribol. Lett. **53**(3), 543–554 (2014)
61. Spear, J.C., Ewers, B.W., Batteas, J.D.: 2D-nanomaterials for controlling friction and wear at interfaces. Nano Today. **10**(3), 301–314 (2015)
62. Rohatgi, P.K.: Metal matrix composites. Def. Sci. J. **43**(4), 323 (1993)
63. Liu, Y., Rohatgi, P.K., Ray, S.: Tribological characteristics of aluminum-50 vol pct graphite composite. Metall. Trans. A. **24**(1), 151–159 (1993)
64. Rohatgi, P.K., Ray, S., Liu, Y.: Tribological properties of metal matrix-graphite particle composites. Int. Mater. Rev. **37**, 129 (1992)
65. Rohatgi, P.K., et al.: A surface-analytical study of tribodeformed aluminum alloy 319-10 vol. % graphite particle composite. Mater. Sci. Eng. A. **123**(2), 213–218 (1990)
66. Jha, A., et al.: Aluminium alloy-solid lubricant talc particle composites. J. Mater. Sci. **21**(10), 3681–3685 (1986)
67. Bowden, F., Shooter, K.: Frictional behaviour of plastics impregnated with molybdenum disulphide. Res. Appl. Ind. **3**, 384 (1950)
68. Lancaster, J.: Composite self-lubricating bearing materials. Proc. Inst. Mech. Eng. **182**(1), 33–54 (1967)
69. Prasad, S., Mecklenburg, K.R.: Self-lubricating aluminum metal-matrix composites dispersed with tungsten disulfide and silicon carbide. Lubr. Eng. **50**(7), 511 (1994)
70. Das, S., Prasad, S.V., Ramachandran, T.R.: Tribology of Al-Si alloy-graphite composites: triboinduced graphite films and the role of silicon morphology. Mater. Sci. Eng. A. **138**(1), 123–132 (1991)
71. Das, S., Prasad, S.V., Ramachandran, T.R.: Microstructure and wear of cast (Al-Si alloy)-graphite composites. Wear. **133**(1), 173–187 (1989)
72. Gibson, P.R., Clegg, A.J., Das, A.A.: Wear of cast Al-Si alloys containing graphite. Wear. **95** (2), 193–198 (1984)
73. Biswas, S.K., Bai, B.N.P.: Dry wear of Al-graphite particle composites. Wear. **68**(3), 347–358 (1981)
74. Jha, A.K., Prasad, S.V., Upadhyaya, G.S.: Sintered 6061 aluminium alloy – solid lubricant particle composites: sliding wear and mechanisms of lubrication. Wear. **133**(1), 163–172 (1989)

75. Akhlaghi, F., Mahdavi, S.: Effect of the SiC content on the tribological properties of hybrid Al/Gr/SiC composites processed by in situ powder metallurgy (IPM) method. Adv. Mater. Res. **264–265**, 1878–1886 (2011)
76. Maurya, R., et al.: Effect of carbonaceous reinforcements on the mechanical and tribological properties of friction stir processed Al6061 alloy. Mater. Des. **98**, 155–166 (2016)
77. Sarmadi, H., Kokabi, A., Reihani, S.S.: Friction and wear performance of copper–graphite surface composites fabricated by friction stir processing (FSP). Wear. **304**(1), 1–12 (2013)
78. Soleymani, S., Abdollah-Zadeh, A., Alidokht, S.: Microstructural and tribological properties of Al5083 based surface hybrid composite produced by friction stir processing. Wear. **278**, 41–47 (2012)
79. Dolatkhah, A., et al.: Investigating effects of process parameters on microstructural and mechanical properties of Al5052/SiC metal matrix composite fabricated via friction stir processing. Mater. Des. **37**, 458–464 (2012)
80. Alidokht, S.A., et al.: Microstructure and tribological performance of an aluminium alloy based hybrid composite produced by friction stir processing. Mater. Des. **32**(5), 2727–2733 (2011)
81. Gan, Y., Solomon, D., Reinbolt, M.: Friction stir processing of particle reinforced composite materials. Materials. **3**(1), 329 (2010)
82. Chen, L.-Y., et al.: Novel nanoprocessing route for bulk graphene nanoplatelets reinforced metal matrix nanocomposites. Scr. Mater. **67**(1), 29–32 (2012)
83. Nickchi, T., Ghorbani, M.: Pulsed electrodeposition and characterization of bronze-graphite composite coatings. Surf. Coat. Technol. **203**(20), 3037–3043 (2009)
84. Algul, H., et al.: The effect of graphene content and sliding speed on the wear mechanism of nickel-graphene nanocomposites. Appl. Surf. Sci. **359**, 340–348 (2015)
85. Uysal, M., et al.: Structural and sliding wear properties of Ag/Graphene/WC hybrid nanocomposites produced by electroless co-deposition. J. Alloys Compd. **654**, 185–195 (2016)
86. Pialago, E.J.T., Kwon, O.K., Park, C.W.: Cold spray deposition of mechanically alloyed ternary Cu–CNT–SiC composite powders. Ceram. Int. **41**(5), 6764–6775 (2015)
87. Pialago, E.J.T., Park, C.W.: Cold spray deposition characteristics of mechanically alloyed Cu-CNT composite powders. Appl. Surf. Sci. **308**, 63–74 (2014)
88. Cho, S., et al.: Multi-walled carbon nanotube-reinforced copper nanocomposite coating fabricated by low-pressure cold spray process. Surf. Coat. Technol. **206**(16), 3488–3494 (2012)
89. Bakshi, S.R., et al.: Nanoscratch behavior of carbon nanotube reinforced aluminum coatings. Thin Solid Films. **518**(6), 1703–1711 (2010)
90. Bakshi, S.R., et al.: Deformation and damage mechanisms of multiwalled carbon nanotubes under high-velocity impact. Scr. Mater. **59**(5), 499–502 (2008)
91. Bakshi, S.R., et al.: Carbon nanotube reinforced aluminum composite coating via cold spraying. Surf. Coat. Technol. **202**(21), 5162–5169 (2008)
92. Chen, Y., Bakshi, S.R., Agarwal, A.: Correlation between nanoindentation and nanoscratch properties of carbon nanotube reinforced aluminum composite coatings. Surf. Coat. Technol. **204**(16), 2709–2715 (2010)
93. Pialago, E.J.T., et al.: Ternary Cu–CNT–AlN composite coatings consolidated by cold spray deposition of mechanically alloyed powders. J. Alloys Compd. **650**, 199–209 (2015)
94. Pialago, E.J.T., Kwon, O.K., Park, C.W.: Nucleate boiling heat transfer of R134a on cold sprayed CNT–Cu composite coatings. Appl. Therm. Eng. **56**(1), 112–119 (2013)
95. Rajkumar, K., Aravindan, S.: Tribological performance of microwave sintered copper–TiC–graphite hybrid composites. Tribol. Int. **44**(4), 347–358 (2011)
96. Rajkumar, K., Aravindan, S.: Tribological studies on microwave sintered copper–carbon nanotube composites. Wear. **270**(9), 613–621 (2011)
97. Rajkumar, K., Aravindan, S.: Tribological behavior of microwave processed copper–nanographite composites. Tribol. Int. **57**, 282–296 (2013)

98. Mogonye, J.E., et al.: Solid/self-lubrication mechanisms of an additively manufactured Ni–Ti–C metal matrix composite. Tribol. Lett. **64**(3), 37 (2016)
99. Esawi, A.M.K., et al.: Fabrication and properties of dispersed carbon nanotube–aluminum composites. Mater. Sci. Eng. A. **508**(1–2), 167–173 (2009)
100. Kim, K.T., Cha, S.I., Hong, S.H.: Hardness and wear resistance of carbon nanotube reinforced Cu matrix nanocomposites. Mater. Sci. Eng. A. **449–451**, 46–50 (2007)
101. Dong, S.R., Tu, J.P., Zhang, X.B.: An investigation of the sliding wear behavior of Cu-matrix composite reinforced by carbon nanotubes. Mater. Sci. Eng. A. **313**(1–2), 83–87 (2001)
102. Tjong, S.C.: Recent progress in the development and properties of novel metal matrix nanocomposites reinforced with carbon nanotubes and graphene nanosheets. Mater. Sci. Eng. R. Rep. **74**(10), 281–350 (2013)
103. Scharf, T., et al.: Self-lubricating carbon nanotube reinforced nickel matrix composites. J. Appl. Phys. **106**(1), 013508 (2009)
104. Zhou, S.-m., et al.: Fabrication and tribological properties of carbon nanotubes reinforced Al composites prepared by pressureless infiltration technique. Compos. A Appl. Sci. Manuf. **38** (2), 301–306 (2007)
105. Hu, Z., et al.: Laser sintered single layer graphene oxide reinforced titanium matrix nanocomposites. Compos. Part B Eng. **93**, 352–359 (2016)
106. Zhai, W., et al.: Investigation of mechanical and tribological behaviors of multilayer graphene reinforced Ni_3Al matrix composites. Compos. Part B Eng. **70**, 149–155 (2015)
107. Bastwros, M., et al.: Effect of ball milling on graphene reinforced Al6061 composite fabricated by semi-solid sintering. Compos. Part B Eng. **60**, 111–118 (2014)
108. Ghazaly A., Seif B., Salem H.G.: Mechanical and Tribological Properties of AA2124-Graphene Self Lubricating Nanocomposite. In: Sadler B.A. (ed.) Light Metals 2013. The Minerals, Metals & Materials Series. Springer, Cham (2013)
109. Tyagi, R., et al.: Elevated temperature tribological behavior of Ni based composites containing nano-silver and hBN. Wear. **269**(11), 884–890 (2010)
110. Selvakumar, N., Narayanasamy, P.: Optimization and effect of weight fraction of MoS_2 on the tribological behaviour of Mg-TiC-MoS_2 hybrid composites. Tribol. Trans. **59**(4), 733–747 (2016)
111. Kato, H., et al.: Wear and mechanical properties of sintered copper–tin composites containing graphite or molybdenum disulfide. Wear. **255**(1), 573–578 (2003)
112. Du, L., et al.: Preparation and wear performance of NiCr/Cr_3C_2–NiCr/hBN plasma sprayed composite coating. Surf. Coat. Technol. **205**(12), 3722–3728 (2011)
113. Yuan, J., et al.: Fabrication and evaluation of atmospheric plasma spraying WC–Co–Cu–MoS_2 composite coatings. J. Alloys Compd. **509**(5), 2576–2581 (2011)
114. Liu, X.-B., et al.: Development and characterization of laser clad high temperature self-lubricating wear resistant composite coatings on Ti–6Al–4V alloy. Mater. Des. **55**, 404–409 (2014)
115. Yan, H., et al.: Laser cladding of Co-based alloy/TiC/CaF_2 self-lubricating composite coatings on copper for continuous casting mold. Surf. Coat. Technol. **232**, 362–369 (2013)
116. Zhang, Y., et al.: Cold-sprayed Cu-MoS_2 and its fretting wear behavior. J. Therm. Spray Technol. **25**(3), 473–482 (2016)
117. Neshastehriz, M., et al.: On the bonding mechanism in cold spray of deformable hex-BN-Ni clusters. J. Therm. Spray Technol. **25**(5), 982–991 (2016)
118. Smid, I., et al.: Cold-sprayed Ni-hBN self-lubricating coatings. Tribol. Trans. **55**(5), 599–605 (2012)
119. Moridi, A., et al.: Cold spray coating: review of material systems and future perspectives. Surf. Eng. **30**(6), 369–395 (2014)
120. Hou, X., et al.: Preparation and properties of hexagonal boron nitride fibers used as high temperature membrane filter. Mater. Res. Bull. **49**, 39–43 (2014)
121. Bi, Q., S. Zhu, and W. Liu, High Temperature Self-Lubricating Materials. In: Pihtili H. (ed.) Tribology in Engineering, pp.109–134. InTech, Rijeka (2013)

122. Kovalchenko, A., Fushchich, O., Danyluk, S.: The tribological properties and mechanism of wear of Cu-based sintered powder materials containing molybdenum disulfide and molybdenum diselenite under unlubricated sliding against copper. Wear. **290**, 106–123 (2012)
123. Furlan, K.P., et al.: Influence of alloying elements on the sintering thermodynamics, microstructure and properties of Fe–MoS_2 composites. J. Alloys Compd. **652**, 450–458 (2015)
124. Mahathanabodee, S., et al.: Comparative studies on wear behaviour of sintered 316L stainless steels loaded with h-BN and MoS_2. Adv. Mater. Res. **747**, 307 (2013). Trans Tech Publ
125. Mahathanabodee, S., et al.: Effects of hexagonal boron nitride and sintering temperature on mechanical and tribological properties of SS316L/h-BN composites. Mater. Des. **46**, 588–597 (2013)
126. Mahathanabodee, S., et al.: Effect of h-BN content on the sintering of SS316L/h-BN composites. Adv. Mater. Res. **410**, 216–219 (2012)
127. Shi, X., et al.: Tribological behavior of Ni_3Al matrix self-lubricating composites containing WS_2, Ag and hBN tested from room temperature to 800 °C. Mater. Des. **55**, 75–84 (2014)
128. Cardenas, A., et al.: Effect of glow discharge sintering in the properties of a composite material fabricated by powder metallurgy. J. Phys. Conf. Ser. **687**(1), p. 012025 (2016)
129. Quazi, M., et al.: A review to the laser cladding of self-lubricating composite coatings. Lasers Manuf. Mater. Process. **3**(2), 67–99 (2016)
130. Xu, J., Liu, W., Zhong, M.: Microstructure and dry sliding wear behavior of MoS_2/TiC/Ni composite coatings prepared by laser cladding. Surf. Coat. Technol. **200**(14–15), 4227–4232 (2006)
131. Lei, Y., et al.: Microstructure and phase transformations in laser clad CrxSy/Ni coating on H13 steel. Opt. Lasers Eng. **66**, 181–186 (2015)
132. Zhang, S., et al.: Friction and wear behavior of laser cladding Ni/hBN self-lubricating composite coating. Mater. Sci. Eng. A. **491**(1), 47–54 (2008)
133. Zhu, S., et al.: Ni_3Al matrix high temperature self-lubricating composites. Tribol. Int. **44**(4), 445–453 (2011)
134. Liu, X.-B., et al.: Effects of temperature and normal load on tribological behavior of nickel-based high temperature self-lubricating wear-resistant composite coating. Compos. Part B Eng. **53**, 347–354 (2013)
135. Wang, A., et al.: Ni-based alloy/submicron WS_2 self-lubricating composite coating synthesized by Nd: YAG laser cladding. Mater. Sci. Eng. A. **475**(1), 312–318 (2008)
136. Liu, X.-B., et al.: Microstructure and wear behavior of γ/Al_4C_3/TiC/CaF_2 composite coating on γ-TiAl intermetallic alloy prepared by Nd:YAG laser cladding. Appl. Surf. Sci. **255**(11), 5662–5668 (2009)
137. Liu, W.-G., et al.: Development and characterization of composite Ni–Cr–C–CaF_2 laser cladding on γ-TiAl intermetallic alloy. J. Alloys Compd. **470**(1), L25–L28 (2009)
138. Papyrin, A.: 2 – The development of the cold spray process A2. In: Champagne, V.K. (ed.) The Cold Spray Materials Deposition Process, pp. 11–42. Woodhead Publishing, Cambridge, England (2007)
139. Du, H., et al.: Structure, mechanical and sliding wear properties of WC–Co/MoS_2–Ni coatings by detonation gun spray. Mater. Sci. Eng. A. **445**, 122–134 (2007)
140. Du, H., et al.: Fabrication and evaluation of D-gun sprayed WC–Co coating with self-lubricating property. Tribol. Lett. **23**(3), 261–266 (2006)
141. Du, L., et al.: Effect of NiCr clad BaF_2·CaF_2 addition on wear performance of plasma sprayed chromium carbide-nichrome coating. J. Therm. Spray Technol. **19**(3), 551–557 (2010)
142. Du, L., et al.: Preparation and characterization of plasma sprayed Ni_3Al–hBN composite coating. Surf. Coat. Technol. **205**(7), 2419–2424 (2010)
143. Sahraeinejad, S., et al.: Fabrication of metal matrix composites by friction stir processing with different particles and processing parameters. Mater. Sci. Eng. A. **626**, 505–513 (2015)
144. Aruri, D., et al.: Wear and mechanical properties of 6061-T6 aluminum alloy surface hybrid composites [(SiC + Gr) and (SiC + Al_2O_3)] fabricated by friction stir processing. J. Mater. Res. Technol. **2**(4), 362–369 (2013)

145. Klinkov, S.V., Kosarev, V.F., Rein, M.: Cold spray deposition: significance of particle impact phenomena. Aerosp. Sci. Technol. **9**(7), 582–591 (2005)
146. Champagne, V.K.: 1 – Introduction. In: The Cold Spray Materials Deposition Process, pp. 1–7. Woodhead Publishing, Cambridge, England (2007)
147. Papyrin, A.N.: Preface. In: Cold Spray Technology, pp. x–xii. Elsevier, Oxford (2007)
148. Assadi, H., et al.: Bonding mechanism in cold gas spraying. Acta Mater. **51**(15), 4379–4394 (2003)
149. Papyrin, A., et al.: Chapter 1 – Discovery of the cold spray phenomenon and its basic features. In: Cold Spray Technology, pp. 1–32. Elsevier, Oxford (2007)
150. Botef, I., Villafuerte, J.: Overview. In: Villafuerte, J. (ed.) Modern Cold Spray: Materials, Process, and Applications, pp. 1–29. Springer International Publishing, Cham (2015)
151. Stark, L., et al.: Self-lubricating cold-sprayed coatings utilizing microscale nickel-encapsulated hexagonal boron nitride. Tribol. Trans. **55**(5), 624–630 (2012)
152. Moghadam, A.D., et al.: Mechanical and tribological properties of self-lubricating metal matrix nanocomposites reinforced by carbon nanotubes (CNTs) and graphene – a review. Compos. Part B Eng. **77**, 402–420 (2015)
153. Wang, J., et al.: Reinforcement with graphene nanosheets in aluminum matrix composites. Scr. Mater. **66**(8), 594–597 (2012)
154. Bartolucci, S.F., et al.: Graphene–aluminum nanocomposites. Mater. Sci. Eng. A. **528**(27), 7933–7937 (2011)
155. Stankovich, S., et al.: Graphene-based composite materials. Nature. **442**(7100), 282–286 (2006)
156. Rafiee, M.A., et al.: Enhanced mechanical properties of nanocomposites at low graphene content. ACS Nano. **3**(12), 3884–3890 (2009)
157. Xue, B., et al.: Microstructure and functional mechanism of friction layer in Ni_3Al matrix composites with graphene nanoplatelets. J. Mater. Eng. Perform. **25**(10), 4126–4133 (2016)
158. Chmielewski, M., et al.: Tribological behaviour of copper-graphene composite materials. Key Eng. Mater. **674**, 219–224 (2016)
159. Chen, F., et al.: Effects of graphene content on the microstructure and properties of copper matrix composites. Carbon. **96**, 836–842 (2016)
160. Moghadam, A.D., et al.: Functional metal matrix composites: self-lubricating, self-healing, and nanocomposites-an outlook. JOM. **66**(6), 872–881 (2014)
161. Akhlaghi, F., Zare-Bidaki, A.: Influence of graphite content on the dry sliding and oil impregnated sliding wear behavior of Al2024–graphite composites produced by in situ powder metallurgy method. Wear. **266**(1–2), 37–45 (2009)
162. Akhlaghi, F., Pelaseyyed, S.A.: Characterization of aluminum/graphite particulate composites synthesized using a novel method termed "in-situ powder metallurgy". Mater. Sci. Eng. A. **385** (1–2), 258–266 (2004)
163. Ravindran, P., et al.: Investigation of microstructure and mechanical properties of aluminum hybrid nano-composites with the additions of solid lubricant. Mater. Des. **51**, 448–456 (2013)
164. Suresha, S., Sridhara, B.K.: Wear characteristics of hybrid aluminium matrix composites reinforced with graphite and silicon carbide particulates. Compos. Sci. Technol. **70**(11), 1652–1659 (2010)
165. Choi, H.J., Lee, S.M., Bae, D.H.: Wear characteristic of aluminum-based composites containing multi-walled carbon nanotubes. Wear. **270**(1–2), 12–18 (2010)
166. Poirier, D., Gauvin, R., Drew, R.A.L.: Structural characterization of a mechanically milled carbon nanotube/aluminum mixture. Compos. A Appl. Sci. Manuf. **40**(9), 1482–1489 (2009)
167. Venkatesan, S., Anthony Xavior, M.: Investigation of aluminum (Al7050) metal matrix composites reinforced with graphene nanoparticles using stir casting process. Int. J. Appl. Eng. Res. **10**(15), 35778–35783 (2015)
168. Baradeswaran, A., Perumal, A.E.: Wear and mechanical characteristics of Al 7075/graphite composites. Compos. Part B Eng. **56**, 472–476 (2014)

169. Riahi, A.R., Alpas, A.T.: The role of tribo-layers on the sliding wear behavior of graphitic aluminum matrix composites. Wear. **251**(1–12), 1396–1407 (2001)
170. Basavarajappa, S., et al.: Influence of sliding speed on the dry sliding wear behaviour and the subsurface deformation on hybrid metal matrix composite. Wear. **262**(7), 1007–1012 (2007)
171. Guo, M.L.T., Tsao, C.Y.A.: Tribological behavior of self-lubricating aluminium/SiC/graphite hybrid composites synthesized by the semi-solid powder-densification method. Compos. Sci. Technol. **60**(1), 65–74 (2000)
172. Ravindran, P., et al.: Tribological behaviour of powder metallurgy-processed aluminium hybrid composites with the addition of graphite solid lubricant. Ceram. Int. **39**(2), 1169–1182 (2013)
173. Shanmughasundaram, P., Subramanian, R.: Wear behaviour of eutectic Al-Si alloy-graphite composites fabricated by combined modified two-stage stir casting and squeeze casting methods. Adv. Mater. Sci. Eng. **2013**, 8 (2013)
174. Goldbaum, D., et al.: Tribological behavior of TiN and Ti (Si,C)N coatings on cold sprayed Ti substrates. Surf. Coat. Technol. **291**, 264–275 (2016)
175. Li, J., et al.: FIB and TEM characterization of subsurfaces of an Al–Si alloy (A390) subjected to sliding wear. Mater. Sci. Eng. A. **421**(1–2), 317–327 (2006)
176. Li, J.L., Xiong, D.S., Huo, M.F.: Friction and wear properties of Ni–Cr–W–Al–Ti–MoS_2 at elevated temperatures and self-consumption phenomena. Wear. **265**(3), 566–575 (2008)
177. Zhang, S., et al.: Preparation and characterization of reactively sintered Ni_3Al–hBN–Ag composite coating on Ni-based superalloy. J. Alloys Compd. **473**(1), 462–466 (2009)
178. Tyagi, R., Xiong, D., Li, J.: Effect of load and sliding speed on friction and wear behavior of silver/h-BN containing Ni-base P/M composites. Wear. **270**(7), 423–430 (2011)
179. Tsuya, Y., Umeda, K., Kitamura, M.: Optimum concentration of solid lubricant in compact. Lubr. Eng. **32**(8), 402–407 (1976)
180. Kumar, P.S., Manisekar, K., Vettivel, S.C.: Effect of extrusion on the microstructure and tribological behavior of copper-tin composites containing MoS_2. Tribol. Trans. **59**(6), 1016–1030 (2016)
181. Rohatgi, P.K., et al.: Tribology of metal matrix composites. In: Menezes, L.P., et al. (eds.) Tribology for Scientists and Engineers: From Basics to Advanced Concepts, pp. 233–268. Springer, New York (2013)
182. Lince, J.R.: Tribology of co-sputtered nanocomposite Au/MoS_2 solid lubricant films over a wide contact stress range. Tribol. Lett. **17**(3), 419–428 (2004)
183. Stoyanov, P., Strauss, H.W., Chromik, R.R.: Scaling effects between micro-and macro-tribology for a Ti–MoS_2 coating. Wear. **274**, 149–161 (2012)
184. Uemura, M., et al.: Effect of friction mechanisms on friction coefficient of MoS_2 in an ultrahigh vacuum. Lubr. Eng. **43**(12), 937–942 (1987)
185. Rupert, T.J., Schuh, C.A.: Sliding wear of nanocrystalline Ni–W: structural evolution and the apparent breakdown of Archard scaling. Acta Mater. **58**(12), 4137–4148 (2010)
186. Rupert, T., et al.: Experimental observations of stress-driven grain boundary migration. Science. **326**(5960), 1686–1690 (2009)
187. Hamilton, G.M.: Explicit equations for the stresses beneath a sliding spherical contact. Proc. Inst. Mech. Eng. C J. Mech. Eng. Sci. **197**(1), 53–59 (1983)
188. Yao, B., Han, Z., Lu, K.: Dry sliding tribological properties and subsurface structure of nanostructured copper at liquid nitrogen temperature. Wear. **301**(1), 608–614 (2013)
189. Kliemann, J.-O., et al.: Formation of cold-sprayed ceramic titanium dioxide layers on metal surfaces. J. Therm. Spray Technol. **20**(1–2), 292–298 (2011)
190. Yamada, M., et al.: Cold spraying of TiO_2 photocatalyst coating with nitrogen process gas. J. Therm. Spray Technol. **19**(6), 1218–1223 (2010)